

NAVAL POSTGRADUATE SCHOOL

Monterey , California



THESIS

D17486

An Investigation Into Backscattered Cross Section
Calibration of an Acoustic Sounder Used for
Analysis of Lower Atmospheric Turbulence

by

David Paul Davison, Jr.

December 1988

Thesis Advisor:

D. L. Walters

Approved for public release; distribution is unlimited.

T241858

REPORT DOCUMENTATION PAGE

REPORT SECURITY CLASSIFICATION UNCLASSIFIED		1b. RESTRICTIVE MARKINGS	
SECURITY CLASSIFICATION AUTHORITY		3 DISTRIBUTION/AVAILABILITY OF REPORT Approved for public release; distribution is unlimited	
DECLASSIFICATION/DOWNGRADING SCHEDULE			
PERFORMING ORGANIZATION REPORT NUMBER(S)		5 MONITORING ORGANIZATION REPORT NUMBER(S)	
NAME OF PERFORMING ORGANIZATION Naval Postgraduate School	6b OFFICE SYMBOL (If applicable) 61	7a NAME OF MONITORING ORGANIZATION Naval Postgraduate School	
ADDRESS (City, State, and ZIP Code) Monterey, California 93943-5000		7b ADDRESS (City, State, and ZIP Code) Monterey, California 93943-5000	
NAME OF FUNDING, SPONSORING ORGANIZATION	8b OFFICE SYMBOL (If applicable)	9 PROCUREMENT INSTRUMENT IDENTIFICATION NUMBER	
ADDRESS (City, State, and ZIP Code)		10. SOURCE OF FUNDING NUMBERS	
		PROGRAM ELEMENT NO	PROJECT NO
		TASK NO	WORK UNIT ACCESSION NO
TITLE (Include Security Classification) AN INVESTIGATION INTO BACKSCATTERED CROSS SECTION CALIBRATION OF AN ACOUSTIC SOUNDER USED FOR ANALYSIS OF LOWER ATMOSPHERIC TURBULENCE			
PERSONAL AUTHOR(S) Walters, David Paul, Jr.			
TYPE OF REPORT Thesis	13b TIME COVERED FROM TO	14 DATE OF REPORT (Year, Month, Day) 1988, December	15 PAGE COUNT 165
SUPPLEMENTARY NOTATION The views expressed in this thesis are those of the author and do not reflect the official policy or position of the Department of Defense or the U.S. Government.			
COSATI CODES		18 SUBJECT TERMS (Continue on reverse if necessary and identify by block number)	
FIELD	GROUP	SUB-GROUP	
ABSTRACT (Continue on reverse if necessary and identify by block number)			
Atmospheric temperature structure fluctuations quantified by C_T^2 degrade the spatial and temporal coherence of electromagnetic and acoustic waves propagating in the atmosphere. A computer controlled atmospheric echosounder developed at the Naval Postgraduate School measures a time averaged C_T^2 profile of the lower atmosphere. Assigning the proper C_T^2 values to the backscattered return signals depends on an accurate calibration of this instrument. Calibration involves determination of the product of the echosounder's transmission efficiency E_t and reception efficiency E_r . This thesis provides a preliminary investigation of a calibration process			
DISTRIBUTION/AVAILABILITY OF ABSTRACT <input checked="" type="checkbox"/> UNCLASSIFIED/UNLIMITED <input type="checkbox"/> SAME AS RPT <input type="checkbox"/> DTIC USERS		21 ABSTRACT SECURITY CLASSIFICATION UNCLASSIFIED	
NAME OF RESPONSIBLE INDIVIDUAL Donald L. Walters		22b TELEPHONE (Include Area Code) (408) 646-2267	22c OFFICE SYMBOL 61We



19. (continued)

using pulsed acoustic energy backscattered from hard spheres. Supporting software calculates the desired product $E_r E_t$ based on an assumption of echosounder efficiency reciprocity. Results of the calibration process investigation indicate this assumption may be invalid. The results also indicate the software performs as intended and that the proposed calibration method possesses sufficient merit to warrant further development.

Approved for public release; distribution is unlimited.

An Investigation Into Backscattered Cross Section Calibration of an
Acoustic Sounder Used for Analysis of Lower Atmospheric Turbulence

by

David Paul Davison, Jr.
Lieutenant, United States Navy
B.S., Texas Agricultural and Mechanical University, 1980

Submitted in partial fulfillment of the
requirements for the degree of

MASTER OF SCIENCE IN PHYSICS

from the

NAVAL POSTGRADUATE SCHOOL
December 1988

Thesis
D17486
C.1

ABSTRACT

Atmospheric temperature structure fluctuations quantified by C_T^2 degrade the spatial and temporal coherence of electromagnetic and acoustic waves propagating in the atmosphere. A computer controlled atmospheric echosounder developed at the Naval Postgraduate School measures a time averaged C_T^2 profile of the lower atmosphere. Assigning the proper C_T^2 values to the backscattered return signals depends on an accurate calibration of this instrument. Calibration involves determination of the product of the echosounder's transmission efficiency E_t and reception efficiency E_r .

This thesis provides a preliminary investigation of a calibration process using pulsed acoustic energy backscattered from hard spheres. Supporting software calculates the desired product $E_r E_t$ based on an assumption of echosounder efficiency reciprocity. Results of the calibration process investigation indicate this assumption may be invalid. The results also indicate the software performs as intended and that the proposed calibration method possesses sufficient merit to warrant further development.

TABLE OF CONTENTS

I. INTRODUCTION	1
II. THEORETICAL BACKGROUND	4
A. C_T^2 REVIEW	4
B. ACOUSTIC RANGE EQUATIONS AND EFFICIENCIES	5
1. One Way Range Equation and $E_t G_o$	6
2. Two Way Range Equation and E_r	9
C. ATTENUATION AND RANGE DETERMINATION	12
1. Attenuation	12
2. Range	15
D. BACKSCATTERED CROSS SECTION DETERMINATION	16
1. Initial Conditions and Assumptions	16
2. The Incident Wave	19
3. Detection Conditions and Assumptions	24
4. The Disturbed Wave	25
5. The Scattered Wave and Its Amplitude	27
6. The Backscattered Cross Section	28

E. SPHERICAL BESSEL FUNCTIONS AND THEIR DERIVATIVES	29
III. CALIBRATION PROCESS AND SOFTWARE	32
A. CALIBRATION SOFTWARE DEVELOPMENT	33
1. Differential Scattering Cross Section Software Development	33
2. Backscattered Cross Section Software Development	44
3. Acoustic Array Efficiency Software Development	47
B. DATA ACQUISITION AND SUPPORTING EQUIPMENT	47
1. Two Way Propagation Path Measurements	48
2. One Way Propagation Path Measurements	56
C. RESULTS	58
IV. CONCLUSIONS AND RECOMMENDATIONS	65
A. CONCLUSIONS	65
B. RECOMMENDATIONS	67
C. SUMMARY	70
APPENDIX A ANECHOIC CHAMBER DESCRIPTION	71
APPENDIX B DIFFERENTIAL SCATTERING CROSS SECTION PROGRAM	72
APPENDIX C BACKSCATTERED CROSS SECTION PROGRAM	95
APPENDIX D ACOUSTIC ARRAY EFFICIENCY PROGRAM	109

APPENDIX E ACOUSTIC ARRAY CALIBRATION DATA	140
A. TWO WAY PROPAGATION PATH DATA	140
B. ONE WAY PROPAGATION PATH DATA	150
LIST OF REFERENCES	152
INITIAL DISTRIBUTION LIST	155

ACKNOWLEDGEMENTS

This thesis was made possible by the perception and competent action of Mr. Stevens, the always cheerful aid of Gail Vaucher, and the long distance assistance of Liz Ugorcak.

Thank you, Dr. Walters, for continued opportunity.

I. INTRODUCTION

The variational effect of wind shears, convection, and temperature gradients on atmospheric density distributions characterize atmospheric turbulence. The temperature structure parameter, C_T^2 , and the index of refraction structure parameter, C_n^2 , quantify two density distributions that arise in acoustic and electromagnetic propagation. [Ref. 1]

The density distributions quantified by C_n^2 and C_T^2 induce phase fluctuations in propagating electromagnetic waves. The density distributions of atmospheric turbulence degrade the spatial and temporal coherences of initially coherent electromagnetic radiation. Similar, more pronounced effects occur in the propagation of acoustic waves. [Ref. 1]

A number of techniques for correcting these problems have been proposed, particularly with respect to electromagnetic propagation. These corrective techniques include the use of modular mirrors [Ref. 2], optical phase conjugation [Ref's. 2 and 3], optical and digital signal processing [Ref. 4], and simple avoidance of turbulent air masses. The appropriate timing of transmissions or suitable location of transmission and reception

facilities accomplishes avoidance [Ref's. 5 and 6]. These techniques can be applied alone or in combinations.

A knowledge of the history of the density or refractive structure along a proposed transmission path is required to effectively employ a number of these compensatory techniques. Time-averaged C_T^2 or C_n^2 profiles characterize this history [Ref's. 1 and 7].

Wroblewski and Weingartner developed and Moxcey refined a high resolution, computer controlled acoustic sounder, or echosounder, system. Their computer controlled echosounder system uses a transmitted pulse of acoustic energy as a probe of atmospheric structure. The interaction of the acoustic wave packet with atmospheric turbulence is used to develop a time-averaged C_T^2 profile for a short spatial range [Ref's. 5, 6 and 8]. The acoustic sounder may also be used to verify certain long range optical measurements of turbulence [Ref. 6].

Development of the C_T^2 profile uses a C_T^2 expression developed from the echosonde equation summarized by Neff [Ref. 7] and the empirical acoustic backscatter cross section per unit volume expression of Tatarski [Ref. 9] [Ref's. 5 and 6]. The accuracy of the absolute values of this C_T^2 profile depends on the calibration of the acoustic antenna parameters

contained in the C_T^2 expression. The antenna parameters of interest are E_t , the efficiency of conversion of electrical to acoustic power, and E_r , the efficiency of conversion of acoustic power to electrical power.

In this thesis acoustic energy backscattered off acoustically hard spheres was used to determine E_r and E_t . Acoustic range equations were software implemented to perform the necessary calculations. Data and calculational results provided first order verification of the calibration process.

II THEORETICAL BACKGROUND

A. C_T^2 REVIEW

Wroblewski and Weingartner applied the echosonde equation,

$$P_r = E_r [P_t E_t] [e^{-2\alpha R}] \left[\frac{C\tau}{2} \sigma_0(R, f) \right] \left[\frac{A}{R^2} G \right], \quad (1)$$

summarized by Neff [Ref. 7] and the acoustic backscattering cross section per unit volume expression given by Tatarski [Ref. 9] as

$$\sigma_0(R, f) = 0.0039 k^{1/3} \frac{C_T^2}{T_0^2} \quad (2)$$

to develop the volume averaged expression

$$C_T^2 = \frac{1}{0.0039} \frac{1}{E_r E_t} \frac{T_0^2}{k^{1/3}} \frac{2}{C\tau} \frac{1}{AG} \frac{P_r}{P_t} R^2 e^{2\alpha R}, \quad (3)$$

where

- P_r is the electrical power of the reflected signal returned to the acoustical antenna array,
- E_r is the efficiency of conversion of the returned acoustic power to P_r ,
- P_t is the electrical power supplied to the acoustical array,
- E_t is the efficiency of conversion of P_t to acoustic power,
- α is the average attenuation per unit distance along the transmission path,
- R is the range from the array to the target or backscattering volume,

- c is the average speed of sound along the transmission path,
- τ is the length in time of the transmitted acoustic pulse,
- A is the antenna's aperture area,
- G is the antenna's effective aperture factor,
- k is the wavenumber of the incident acoustic energy, and
- T_0 is the average temperature (in degrees Kelvin) along the transmission path.

[Ref's. 5 and 6]

The conditions at the time and location of each application determine the value of the terms T_0 , k , c , τ , P_r , P_t , R and α in the C_T^2 expression.

The terms A and G depend on the antenna design.

Adverse field effects such as dust, debris and vibration loosened connections cause the remaining two terms, E_r and E_t , to change over the life of the system. This chapter develops the theoretical expressions supporting a determination of E_r and E_t .

B. ACOUSTIC RANGE EQUATIONS AND EFFICIENCIES

In the following two sections the acoustic range equation of Neff [Ref. 7] is re-developed for targets of small area relative to the cross-section of the ensonifying field. Neff [Ref. 7], Skolnik [Ref. 10], and Probert-Jones [Ref. 11] were used for guidance.

1. One Way Range Equation and $E_t G_0$

As defined previously, the electrical power supplied to the acoustic array is P_t . It is converted at an efficiency E_t to an emitted acoustic power,

$$P_a = P_t E_t . \quad (4)$$

P_a is spread over a 4π solid angle.

A far field range R is defined by the condition

$$\lambda/2 \gg |L| - |R| \quad (5)$$

for the geometry in Figure 1. λ is the wavelength of the emitted acoustic wave.

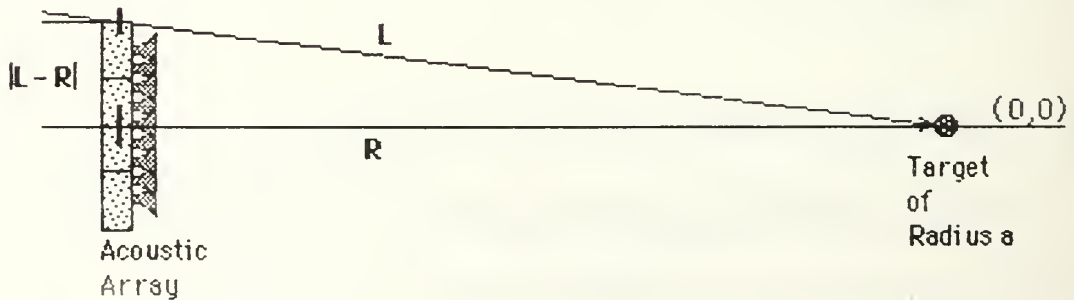


Figure 1: Calibration (Far Field) Geometry

The acoustic intensity,

$$I_a = P_a / 4\pi R^2, \quad (6)$$

describes the emitted acoustic power density of an isotropic emitter at a far field range R . I_a is in units of $[W/m^2]$.

If the emitted power is directional, the intensity I_a is modulated by a geometrical gain,

$$G(\Omega) = G_0 |F(\Omega)|^2 = G_0 |F(\theta, \phi)|^2. \quad (7)$$

Note this is not the same G found in equation (1). Now,

$$|F(0,0)|^2 = 1, \quad (8)$$

and G_0 is therefore the centerline gain of the acoustic array. [Ref. 11] The centerline direction $(0,0)$ is taken to be normal to the face of the acoustic array. The acoustic intensity I_a is now written

$$I_a = \frac{P_a}{4\pi R^2} G(\Omega). \quad (9)$$

In a real propagating medium intensity attenuation occurs along the transmission path. The radial term $e^{-\alpha R}$ accounts for this attenuation when the atmospheric path is assumed to be reasonably

homogeneous. The acoustic intensity is then

$$I_a = \frac{P_a}{4\pi R^2} G(\Omega) e^{-\alpha R}. \quad (10)$$

A target of cross sectional area A_{tgt} intercepts a power

$$P_{tgt} = I_a A_{tgt}. \quad (11)$$

Expanding this expression with equation (10) yields

$$P_{tgt} = \left[\frac{P_a}{4\pi} \right] \left[e^{-\alpha R} G(\Omega) \right] \left[\frac{A_{tgt}}{R^2} \right]. \quad (12)$$

For a target of cross sectional area A_{tgt} with a sufficiently small solid angle A_{tgt}/R^2 little change in intensity occurs about the direction Ω . Equation (12) is now arranged as a one way range equation along the centerline direction (0,0);

$$R = \left[\frac{P_t E_t}{4\pi} e^{-\alpha R} G_0 \frac{A_{tgt}}{P_{tgt}} \right]^{\frac{1}{2}}. \quad (13)$$

Isolating $E_t G_0$ in the above expression yields

$$E_t G_0 = \frac{4\pi R^2}{P_t} e^{\alpha R} \frac{P_{tgt}}{A_{tgt}}. \quad (14)$$

Electrical power is expressed as

$$P = \frac{V_{rms}^2}{Z} = \frac{V_{ms}}{Z} \quad (15)$$

where

- V_{rms} is the empirical root mean square voltage,
- V_{ms} is V_{rms}^2 , and
- Z is the electrical impedance.

$E_t G_0$ is now written

$$E_t G_0 = 4\pi R^2 \frac{Z}{(V_{ms})_t} e^{\alpha R} \frac{P_{tgt}}{A_{tgt}} \quad (16)$$

The ratio P_{tgt}/A_{tgt} is defined as the acoustic intensity I_r

received by the target. Therefore,

$$E_t G_0 = 4\pi R^2 \frac{Z}{(V_{ms})_t} e^{\alpha R} I_r \quad (17)$$

2. Two Way Range Equation and E_r

For an acoustically hard target the total power reflected is P_{tgt} .

The power reflected from the target surface has a normalized, directional intensity distribution described by the differential scattering cross section, σ .

The direction from the target to the array is the backscattered direction. The differential scattering cross section in the backscattered direction is called the normalized backscattered cross section, σ_b . σ_b is defined as the power reflected toward the source per unit solid angle, normalized by the incident power density over a 4π solid angle.

The backscattered intensity from the target is

$$I_{tgt} = \frac{P_{tgt}}{4\pi R^2} \sigma_b . \quad (18)$$

An array of aperture area A at range R intercepts an attenuated, received acoustic power,

$$P_{ra} = I_{tgt} A e^{-\alpha R} . \quad (19)$$

Substituting equation (18) into equation (19) yields

$$P_{ra} = \frac{P_{tgt}}{4\pi R^2} \sigma_b e^{-\alpha R} A . \quad (20)$$

P_{ra} is converted to returned electrical power, P_r , at a return efficiency, E_r ;

$$P_r = P_{ra} E_r . \quad (21)$$

Since electrical power is expressed as

$$P = \frac{V_{rms}^2}{Z} = \frac{V_{ms}}{Z} \quad (15)$$

electrical power representing the returned acoustic signal from a target placed along an emitter's direction (0,0) is written as

$$\frac{(V_{ms})_r}{Z_r} = \frac{(V_{ms})_t}{Z_t} \left[\frac{E_t G_0}{4\pi} e^{-\alpha R} \frac{A_{tgt}}{R^2} \right] \left[\frac{E_r \sigma_b}{4\pi} e^{-\alpha R} \frac{A}{R^2} \right] \quad (22)$$

For a passive, linear acoustic array circuit the concept of impedance reciprocity is invoked [Ref. 12] to yield a two way range equation for scattering from a small target;

$$R = \left[\frac{(V_{ms})_t}{(V_{ms})_r} E_t E_r \frac{G_0 \sigma_b}{(4\pi)^2} e^{-2\alpha R} A A_{tgt} \right]^{\frac{1}{4}} \quad (23)$$

This is written to isolate E_r ;

$$E_r = \frac{(V_{ms})_r}{(V_{ms})_t} \frac{(4\pi R^2)^2}{E_t G_0} \frac{e^{2\alpha R}}{A A_{tgt}} \frac{1}{\sigma_b} \quad (24)$$

A part of the return signal's power is unwanted noise.

Subtracting noise power from the returned acoustic power yields

$$E_r = \frac{(V_{ms})_r - (V_{ms})_n}{(V_{ms})_t} \frac{(4\pi R^2)^2}{E_t G_0} \frac{e^{2\alpha R}}{A A_{tgt}} \frac{1}{\sigma_b} \quad (25)$$

As return voltages are quite small they are analyzed after electrical amplification. Calling the electrical amplification a gain G_e allows introduction of the final modification to E_r :

$$E_r = \frac{(V_{ms})_r - (V_{ms})_n}{(V_{ms})_t G_e^2} \frac{(4\pi R^2)^2}{E_t G_0} \frac{e^{2\alpha R}}{A A_{tgt}} \frac{1}{\sigma_b} . \quad (26)$$

C. ATTENUATION AND RANGE DETERMINATION

Employing equations (17) and (26) in the calibration process requires calculating the attenuation α and the range R from the array to the target.

1. Attenuation

The calculated attenuation α for an atmospheric propagation path is assumed to be the combined result of molecular and classical absorption in the atmosphere. The classical absorption α_{cl} is attributed to heat conduction and viscous effects while the larger molecular absorption α_{mol} is attributed to the excitation of internal energy modes of atmospheric gases by the propagating sound energy. [Ref. 7]

Information from Neff [Ref. 7], Businger [Ref. 13], Neiburger [Ref. 14], and Fuller [Ref. 15] is applied to make a reasonable determination of α . The determination is made using the average measured temperature

T_c in degrees Celsius along the propagation path, the measured atmospheric pressure P in millibars, and the measured relative humidity Rh in percent.

The molecular attenuation coefficient, α_{mol} , is expressed by the empirical relationship

$$\alpha_{mol} = \frac{\alpha_{max}}{304.8} \left[(0.18 f_{ratio})^2 + \left(\frac{2(f_{ratio})^2}{1 + f_{ratio}^2} \right)^2 \right]^{\frac{1}{2}}. \quad (27)$$

α_{mol} is in units of [-dB/m].

Now,

$$\alpha_{max} = 0.0078 f_m (T^*)^{-2.5} e^{7.77(1-1/T^*)} \quad (28)$$

is the maximum absorption at

$$f_m = \frac{(10 + 6600 (100 \frac{e}{P}) + 44,400 (100 \frac{e}{P})^2) P^*}{(T^*)^{0.8}}. \quad (29)$$

f_m is in units of [Hz].

Also,

$$\frac{e}{P} = \frac{E_s Rh}{P - E_s(1 + Rh)} \quad (30)$$

is the mole ratio of water vapor in the atmosphere. The water vapor pressure e is expressed in millibars.

$$E_s = 10^{(9.4 - 2353/T_o)} \quad (31)$$

expresses the saturation vapor pressure E_s . T_o is the average absolute temperature along the transmission path, as defined in Section A.

$$T^* = (1.8 T_c + 492) / 519 , \quad (32)$$

and

$$p^* = p / 1014 . \quad (33)$$

Finally,

$$f_{ratio} = f / f_m , \quad (34)$$

where f is the operating frequency of the echosounder in [Hz]. [Ref's. 7, 13, 14 and 15]

The classical attenuation coefficient, α_{cl} , is approximated by

$$\alpha_{cl} = 1.74 * 10^{-10} (f)^2 . \quad (35)$$

α_{cl} is in units of [-dB/m]. [Ref. 7]

For a total attenuation

$$\alpha_T = \alpha_{cl} + \alpha_{mol} \quad (36)$$

and the relationship

$$- \alpha_T R = 10 \log e^{-\alpha R} \quad (37)$$

the average attenuation per meter is finally written as

$$\alpha = \frac{\alpha_{cl} + \alpha_{mol}}{10} \ln 10 \quad (38)$$

Equation (37) is derived from unit definitions and equation one of Neff [Ref. 7].

2. Range

The coordinate system for the backscattered cross section determination uses the center of the target spheres as the coordinate system origin. Therefore, the radius a of a target sphere and the time of return t_r of an acoustic signal from the acoustic echosounder are used to determine the range R from the target to the echosounder;

$$R = \frac{ct_r}{2} + a . \quad (39)$$

c is the average speed of sound along the transmission path, and

$$t_r = t_{receive} - t_{transmit} . \quad (40)$$

For the range of temperatures expected in normal echosounder operation the speed of sound in meter per seconds in dry air is

$$c_{dry} = 20.05 \sqrt{T_0} . \quad (41)$$

For moist air c becomes

$$c = c_{\text{moist}} = c_{\text{dry}} (1 + 0.14 e/P), \quad (42)$$

where e/P is defined in equation (30). [Ref. 1]

D. BACKSCATTERED CROSS SECTION DETERMINATION

Employing equations (17) and (26) in the calibration process also requires calculating σ_b , the backscattered cross section. Recall from Paragraph B.2 that the backscattered cross section is the differential scattering cross section in the direction of the energy source.

1. Initial Conditions and Assumptions

In determining the differential scattering cross section σ it is assumed the incident wave state is unchanged after scattering. That is, for a stationary, acoustically hard target it is assumed

$$k = k_{\text{incident}} = k_{\text{scattered}}, \quad (43)$$

and that incident k has good definition, i.e. the incident wave can be considered monochromatic [Ref. 16].

Selection of acoustically hard spheres as targets further simplifies the determination of the differential scattering cross section solution. This target selection sets the boundary condition at the target

surface as the Neumann boundary condition

$$\frac{\partial V}{\partial n} = 0. \quad (44)$$

V is the velocity potential defined by the acoustic propagation velocity c as

$$c = \nabla V. \quad (45)$$

n lies along the direction normal to the target surface. Also,

$$p = -\rho_0 \frac{\partial V}{\partial t} \quad (46)$$

for the pressure p and rest density ρ_0 of the propagating medium. [Ref. 16].

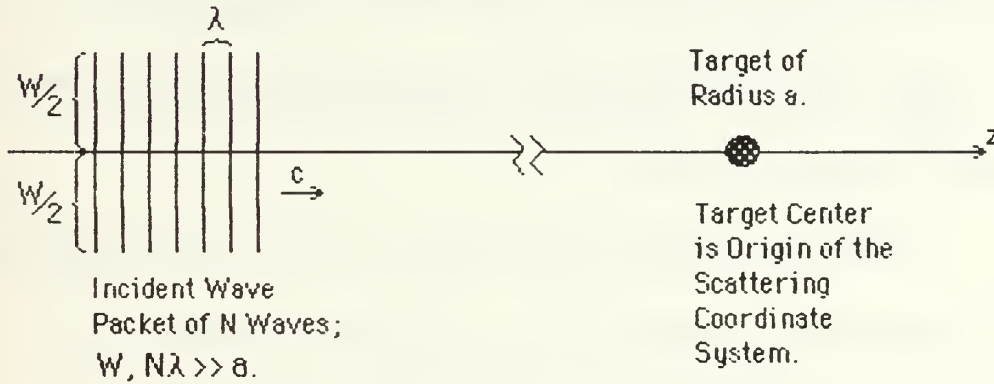


Figure 2: Incident Wave and Target Description

The target sphere is aligned along the centroid of the main acoustic lobe of the acoustic array echosounder, that is, along the direction $(0,0)$, normal to the face of the array. The target sphere is

selected to be sufficiently small with respect to incident beam dimensions so that an essentially uniform intensity is intercepted by the sphere [Ref. 17]. Since the target intercepts a very small proportion of the centroid of the transmitted sounding lobe no accommodation for sounding lobe geometry over the target's angular area is made.

Acoustic gain is simply taken as G_0 .

Target placement is also at a far field range. This allows spherical incident waves to be treated as planar incident waves and places the target outside the range associated with the ring time of the echosounder [Ref. 8]. Placement of the target is also close enough to the array to support an assumption of transmission medium homogeneity along the transmission path.

Finally, the potential describing the target falls off faster than $1/r$. The describing potential for an acoustically hard sphere with radius a is

$$V(\mathbf{r}) = \begin{cases} \infty & r \leq a \\ 0 & r \geq a \end{cases} \quad (47)$$

Thus, for $r > a$ $V(\mathbf{r})$ falls off faster than $1/r$.

Note that with the exception of the specific surface boundary condition for acoustic waves the above conditions and assumptions closely correspond to those for plane electromagnetic waves incident on a perfectly conducting sphere, and for perfectly elastic nuclear scattering in a center of mass coordinate system. [Ref's. 16, 18, 19 and 20]

2. The Incident Wave

The asymptotic form of an incident plane wave approaching a scattering target but beyond the influence of the target's potential $V(\mathbf{r})$ is the undisturbed, or free, plane wave. In the spherical polar coordinates (r, θ, ϕ) illustrated in Figure 3 a free, monochromatic plane wave of unit amplitude propagating in the direction Ω_0 given by (θ_0, ϕ_0) is

$$f(\mathbf{r}, t) = e^{ikr[\cos(\theta_0)\cos(\theta) + \sin(\theta_0)\cos(\theta - \theta_0)]} e^{-i\omega t}. \quad (48)$$

[Ref. 16]

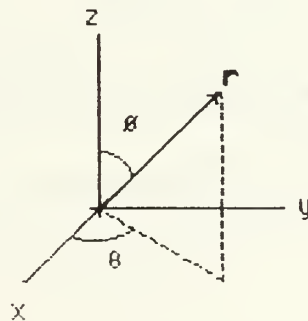


Figure 3: Spherical Polar Coordinates

For a wave of unit amplitude incident along the z axis , $\Omega_0 = 0$

and the free wave $f(\mathbf{r},t)$ is presented as

$$f(\mathbf{r},t) = e^{ikr \cos(\theta)} e^{-i\omega t} = e^{ikz} e^{-i\omega t} . \quad (49)$$

Note this is a solution with axial symmetry for the free wave equation [Ref. 18].

The wave equation describing the behavior of the undisturbed or free monochromatic wave $f(\mathbf{r},t)$ is

$$\left(\nabla^2 - \frac{1}{c^2} \frac{\partial^2}{\partial t^2} \right) f(\mathbf{r},t) = 0 . \quad (50)$$

c is the speed of propagation of the free wave. If the wave function $f(\mathbf{r},t)$ has a simple harmonic time dependence, i.e.,

$$f(\mathbf{r},t) = e^{-i\omega t} f(\mathbf{r}) , \quad (51)$$

then for a wave number

$$k \equiv \omega/c = 2\pi/\lambda \quad (52)$$

the free wave equation becomes the Helmholtz equation

$$[\nabla^2 + k^2] f(\mathbf{r},t) = 0 \quad (53)$$

[Ref. 21].

The stationary solution $\{(\mathbf{r})$ of the free wave equation can be written as the product

$$\{(\mathbf{r}) = \{_1(q_1) \{_2(q_2) \{_3(q_3) \quad (54)$$

for orthogonal curvilinear coordinates q_1, q_2, q_3 [Ref. 16]. Recall an undisturbed plane wave has a cylindrical symmetry about the axis of propagation [Ref. 22]. Using the spherical polar coordinates

$$q_1 = r, \quad q_2 = \vartheta, \quad q_3 = \varphi, \quad (55)$$

the stationary solution describing an undisturbed plane wave propagating along the z axis is

$$\{(\mathbf{r}) = \{_1(r) \{_2(\vartheta) . \quad (56)$$

Substituting $\{(\mathbf{r})$ into the free wave equation expressed in spherical coordinates and separating the coordinate dependencies yields the separated free wave equation,

$$(kr)^2 + \frac{1}{f_1} \frac{d}{dr} r^2 \frac{d}{dr} f_1 = - \frac{1}{f_2 \sin \vartheta} \frac{d}{d\vartheta} (\sin \vartheta \frac{d}{d\vartheta} f_2). \quad (57)$$

Using a separation constant of $l(l+1)$ the equation for the angular dependency of the free wave becomes

$$\frac{1}{f_2 \sin \vartheta} \frac{d}{d\vartheta} (\sin \vartheta \frac{d}{d\vartheta} f_2) + l(l+1) = 0 . \quad (58)$$

Letting

$$\cos(\theta) = x \quad (59)$$

in the angular equation yields

$$\left[(1 - x^2) \frac{d^2}{dx^2} - 2x \frac{d}{dx} + l(l+1) \right] f_2 = 0 . \quad (60)$$

The previous equation is known as the Legendre differential equation [Ref. 21]. The most useful solutions to the Legendre differential equation are the Legendre polynomials, designated by $P_l(x)$. They can be generated by the recursion relationships

$$P_0(x) = 1, \quad (61a)$$

$$P_1(x) = x \quad (61b)$$

and

$$P_l(x) = [2l-1/x] x P_{l-1}(x) - [l-1/x] P_{l-2}(x) \quad (61c)$$

[Ref. 21]. Therefore,

$$f_{2,1}(\theta) = P_1(\cos \theta) . \quad (62)$$

From equation (57), the equation describing the radial dependency of the free wave is

$$\left\{ \frac{d^2}{dr^2} + \frac{2}{r} \frac{d}{dr} + \left[k^2 - \frac{l(l+1)}{r^2} \right] \right\} f_1 = 0 . \quad (63)$$

Changing scale to the variable $s = kr$ yields the differential equation

$$\left\{ \frac{d^2}{ds^2} + \frac{2}{s} \frac{d}{ds} + \left[1 - \frac{1(1+1)}{s^2} \right] \right\} f_1 = 0 \quad (64)$$

[Ref. 17].

This differential equation has the spherical Bessel function $j_1(s)$ with amplitude A_1 as a solution;

$$f_{1,1}(s) = A_1 j_1(s) \quad (65)$$

[Ref. 18].

The stationary solution of the free wave equation in spherical coordinates is now written as the partial wave

$$f_1(r) = P_1(\cos \vartheta) [A_1 j_1(kr)] . \quad (66)$$

The most general form of this free wave equation solution is a Fourier-Bessel series,

$$f(r, \vartheta) = \sum_{l=0}^{\infty} A_l j_l(kr) P_l(\cos \vartheta) \quad (67)$$

[Ref's. 17 and 21].

A plane, free wave of unit amplitude propagating in the direction $\Omega_0 = 0$ is then

$$e^{ikz} = \sum_{l=0}^{\infty} A_l j_l(kr) P_l(\cos \vartheta) . \quad (68)$$

The norm of the Legendre polynomials, the asymptotic expression

$$j_1(kr) \sim \frac{\sin(kr - \frac{\pi}{2})}{kr} \quad (69)$$

and the process detailed in Elton [Ref. 18] are used to determine A_1 ;

$$A_1 = i^1 [2 \cdot 1 + 1] . \quad (70)$$

Therefore,

$$e^{ikz} = \sum_{l=0}^{\infty} i^l [2l + 1] j_l(kr) P_l(\cos \theta) \quad (71)$$

[Ref's. 18 and 21].

3. Detection Conditions and Assumptions

As the dimensions of the incident acoustic wave packet are greater than the size of the target it is expected that a portion of the incident wave packet continues to propagate past the target. The total or disturbed wave description is then a superposition of the incident and scattered wave descriptions. [Ref. 17]

The acoustic array serves as both transmitter and receiver, or detector. This keeps the detector outside the path of continued propagation of the incident wave packet. [Ref. 17] Therefore, only the scattered wave description is of interest in the calibration of the array.

The placement of the target at a far field range simultaneously places the detector in the region of asymptotic behavior of the scattered wave.

4. The Disturbed Wave

Once an incident wave described by the velocity potential $V(r)$ enters the region of influence of a scattering target's spherical potential $V(r)$ the wave equation becomes the disturbed wave equation

$$\{ \nabla^2 + [k^2 - V(r)] \} V(r) = 0 \quad (72)$$

[Ref. 17]. Comparison of the form of the disturbed wave equation to the free wave equation gives an expectation of a solution of the form

$$V(r) = V_1(r) V_2(\theta) . \quad (73)$$

Substituting $V(r)$ into the disturbed wave equation and separating variables yields

$$-\frac{1}{V_2 \sin \theta} \frac{d}{d\theta} \left(\sin \theta \frac{d}{d\theta} \right) V_2 = r^2 [k^2 - V(r)] + \frac{1}{V_1} \frac{d}{dr} r^2 \frac{d}{dr} V_1 . \quad (74)$$

The angular equation for the disturbed wave is identical in form to the angular equation for the free wave and independent of the Neumann boundary condition $\partial V / \partial r = 0$. Therefore,

$$V_{2,1}(\theta) = P_1(\cos \theta) . \quad (75)$$

Using the previous substitution of $s = kr$ yields the now modified Bessel equation as the radial equation for the disturbed wave;

$$\left\{ \frac{d^2}{ds^2} + \frac{2}{s} \frac{d}{ds} + \left[1 - \frac{l(l+1) + V(r)}{s^2} \right] \right\} V_l = 0 . \quad (76)$$

Following the solution development in Elton [Ref. 18] and applying the Neumann boundary condition at $r = a$ leads to a solution

$$V_{1,1}(r) = i^1 [2l + 1] [j_1(kr) - a_1' h_1^{(1)}(kr)] . \quad (77)$$

The relationship

$$a_1' = i e^{-i\delta_1} \sin \delta_1 = \frac{j_1'(ka)}{h_1^{(1)'}(ka)} \quad (78)$$

is defined from Morse [Ref. 17] and Bowman [Ref. 16]. Additionally,

- the $j_l(kr)$ are the spherical Bessel functions of the first kind, argument kr , and order l ,
- $h_l^{(1)}(kr)$ are the Hankel functions of argument kr and order l ,
- the δ_l are the phase shifts of the usual partial wave description for spherical scattering solutions [Ref's. 17 and 20],
- the $j_l'(ka)$ are the first derivatives of the $j_l(kr)$, taken with respect to the argument kr and evaluated at $r = a$,
- $h_l^{(1)'}(ka) = j_l'(ka) + i y_l'(ka)$, and (79)
- the $y_l'(ka)$ are the first derivatives of the $y_l(kr)$, the spherical Bessel functions of the second kind with argument kr and order l , taken with respect to the argument kr and evaluated at $r = a$.

The general series solution for the total disturbed wave $V(\mathbf{r})$ is then

$$V(\mathbf{r}) = \sum_{l=0}^{\infty} i^l [2l + 1] P_l(\cos \theta) [j_l(kr) - a_l' h_l^{(1)}(kr)] . \quad (80)$$

5. The Scattered Wave and Its Amplitude

The general asymptotic form for a disturbed wave $V(r, \Omega)$

resulting from a plane wave $V_i(r, \Omega)$ incident along $\Omega_0 = 0$ and scattered by a spherical potential $V(r)$ is

$$V(r, \Omega) \cong e^{ikz} + s(\Omega) e^{ikr}/r \quad (81)$$

[Ref. 18]. This description of the asymptotic disturbed wave is a superposition of the incident plane wave e^{ikz} and a spherical, scattered wave $s(\Omega)e^{ikr}/r$. The term $s(\Omega)$ is called the scattering amplitude [Ref's. 18, 19 and 22].

Now, recalling the series equivalence for the plane wave incident along Ω_0 in equation (71), and comparing the general series solution for the disturbed wave in equation (80) to its asymptotic form in equation (81) gives

$$s(\Omega)e^{ikr}/r = - \sum_{l=0}^{\infty} i^l [2l + 1] P_l(\cos \theta) a_l' h_l^{(1)}(kr) . \quad (82)$$

This is a series expression for the scattered wave. Therefore,

$$s(\Omega) = \frac{\sqrt{4\pi}}{k} i \sum_{l=0}^{\infty} [2l+1] P_l(\cos \theta) a_l' \quad (83)$$

[Ref's. 16 and 18].

6. The Backscattered Cross Section

The scattering amplitude $s(\Omega)$ is related to the differential scattering cross section $\sigma(\Omega) = \sigma A_{tgt}$ by

$$\sigma(\Omega) = |s(\Omega)|^2 \quad (84)$$

[Ref's. 18, 19 and 22].

Applying the series expression for the scattering amplitude in equation (83) to the previous equation yields

$$\sigma A_{tgt} = \sigma(\Omega) = \frac{4\pi}{k^2} \left| \sum_{l=0}^{\infty} i [2l+1] a_l' P_l(\cos \theta) \right|^2. \quad (85)$$

For the backscattered direction $\theta = \pi$ this gives a backscattered cross section of

$$\sigma_b A_{tgt} = \sigma_B = \frac{4\pi}{k^2} \left| \sum_{l=0}^{\infty} [2l+1] a_l' \right|^2 \quad (86a)$$

[Ref's. 16 and 17]. For the spherical target $A_{tgt} = \pi a^2$, so

$$\sigma_b = \frac{4}{(ka)^2} \left| \sum_{l=0}^{\infty} [2l+1] a_l' \right|^2. \quad (86b)$$

It should be noted a plane wave of unit amplitude incident from the positive z direction and backscattered along $\theta = 0$ would introduce a factor of $(-1)^l$ into the previous sum [Ref. 16].

E. SPHERICAL BESSEL FUNCTIONS AND THEIR DERIVATIVES

Implementation of the previous equation necessitates calculation of the a_l' . The recursion relations

$$j_0'(ka) = [-j_0(ka) + \cos(ka)]/ka, \quad (87a)$$

$$j_1'(ka) = \{-[1 + 1][j_1(ka)]/ka\} + j_{1-1}(ka), \quad (87b)$$

$$y_0'(ka) = [-y_0(ka) + \sin(ka)]/ka \quad (87c)$$

and

$$y_1'(ka) = \{-[1 + 1][y_1(ka)]/ka\} + y_{1-1}(ka) \quad (87d)$$

determine the $j_l'(ka)$ and $y_l'(ka)$ needed for the calculation of a_l' in equation (78) [Ref's. 21 and 23].

Determination of the regular and irregular spherical Bessel functions at $r = a$ supports the use of the recursion relations in equations (87). As ka is real the irregular spherical Bessel functions are stable enough to use the recursion relations

$$y_0(ka) = -[\cos(ka)]/ka, \quad (88a)$$

$$y_1(ka) = [y_0(ka) - \sin(ka)]/ka \quad (88b)$$

and

$$y_l(ka) = \{[2l - 1][y_{l-1}(ka)]/ka\} - y_{l-2}(ka) \quad (88c)$$

in their determination [Ref's. 23 and 24].

Because the size of the argument of the regular spherical Bessel functions may be very small the method of negative continued fractions is appropriate to the fast and accurate determination of a converging solution to these functions [Ref.24]. The regular spherical Bessel function reciprocals are therefore determined by the negative continued fraction calculation

$$\frac{1}{j_l(ka)} = \frac{1}{j_0(ka)} \frac{[-][b_{1,1}][b_{1,2},b_{1,1}]...[b_{l,1}][b_{l,2},b_{l,1}]...}{[b_{1,2}].....[b_{l,2}][b_{l,3},b_{l,2}]...} \quad (89)$$

Now,

$$b_{l,m} = 2(l + m - 1)/ka \quad (90)$$

and

$$\begin{aligned}
 [-](b_{1,m}, \dots, b_{1,2}, b_{1,1}) &= b_{1,m} - \frac{1}{b_{1,m-1}} - \dots - \frac{1}{b_{1,2}} - \frac{1}{b_{1,1}} \\
 &= b_{1,m} - \frac{1}{b_{1,m-1} - \frac{1}{b_{1,m-2} - \frac{1}{b_{1,m-3} - \dots - \frac{1}{b_{1,2} - \frac{1}{b_{1,1}}}}}
 \end{aligned} \tag{91}$$

[Ref. 25].

While the regular spherical Bessel function reciprocal calculation of equation (89) would appear to involve an infinite number of terms, the calculation can in fact be terminated when the m^{th} numerator term equals the m^{th} denominator term to the desired precision for the spherical Bessel function's solution. [Ref's. 24 and 25]

III. CALIBRATION PROCESS AND SOFTWARE

Small quantities of data were collected in the anechoic chamber at the Naval Postgraduate School. This data aided first order verification of the calibration process and its supporting software. A brief description of the anechoic chamber is provided in Appendix A.

The calibration process and data development occurred in two stages. The first stage used equation (26) and two way propagation path measurements to determine $\sigma_b E_r E_t G_0$. The second stage determined $E_t G_0$ using equation (17) and one way propagation path measurements.

E_r was then determined from $\sigma_b E_r E_t G_0$, $E_t G_0$ and the calculated σ_b of equation (86b).

Because reciprocity was assumed for E_r and E_t

$$E_r E_t = E_r^2 \quad (92)$$

provided the desired calibration information.

Supporting software was written to perform calculations required for calibration. The next section describes the development of this software.

A. CALIBRATION SOFTWARE DEVELOPMENT

Calibration software was written in BASIC. It was used with a BASIC 4.0 compiler on a Hewlett Packard 310 computer. Computer performance was enhanced by an Infotek floating point processor.

Notation in the programs sometimes differs from that in the thesis text as a result of H.P. keyboard limitations. Variable definitions are located at the beginning of subprograms or modules. These definitions are provided throughout a program as an aid in determining program to text variable equivalence.

The main effort of software development was calculation of backscattered cross sections. This was done with equation (86b). Information available for summation loop verification was differential scattering cross section information. Differential scattering section software was developed first.

1. Differential Scattering Cross Section Software Development

The differential scattering cross sections σ were calculated using equation (85) and equation (78).

To support equation (78) employment the subprograms calculating the values of the Legendre polynomials and the values of the

regular and irregular spherical Bessel functions were developed first. Each subprogram was developed and tested separately in test programs. Each test program was designed to provide a tabular output for verification against values found in Abramowitz and Stegun [Ref. 23].

The Legendre values were calculated using equations (61). The irregular spherical Bessel functions were calculated using equations (88). The regular spherical Bessel functions were calculated using equations (89), (90) and (91).

Following verification these subprograms were assembled with subprograms calculating the derivatives of the regular and irregular spherical Bessel functions, the normalized differential scattering cross section σ , the scattering modulus of Bowman [Ref. 16], and with three graphics subprograms. This assembly created the differential scattering cross section program found in Appendix B.

The values of the regular and irregular spherical Bessel function derivatives at $r=a$ were calculated using equations (87).

Differential scattering cross sections were calculated using equation (85). The number of orders l required for the summation calculation in equation (85) was determined by generating tabular outputs

and determining the number of orders required for numerical stability to occur to 12 decimal places. This stability process was based on the concept of the phase shift δ_l of each outgoing partial scattered wave becoming progressively smaller with increasing l until a_l' (equation (78)) became negligible for the precision desired [Ref's. 18, 19, 20 and 22].

Tabular outputs covered a ka value range of one to thirty at varying scattering angles, including $\theta = \pi$. This ka value range selection was based on the expected maximum target size to be encountered during actual echosounder employment.

Twenty-one orders greater than the integer value of the argument ka were determined to be required for equation (85)'s summation. The number of orders required was greater than the usually cited relationship

$$ka \approx \sqrt{1(1 + 1)} \quad (93)$$

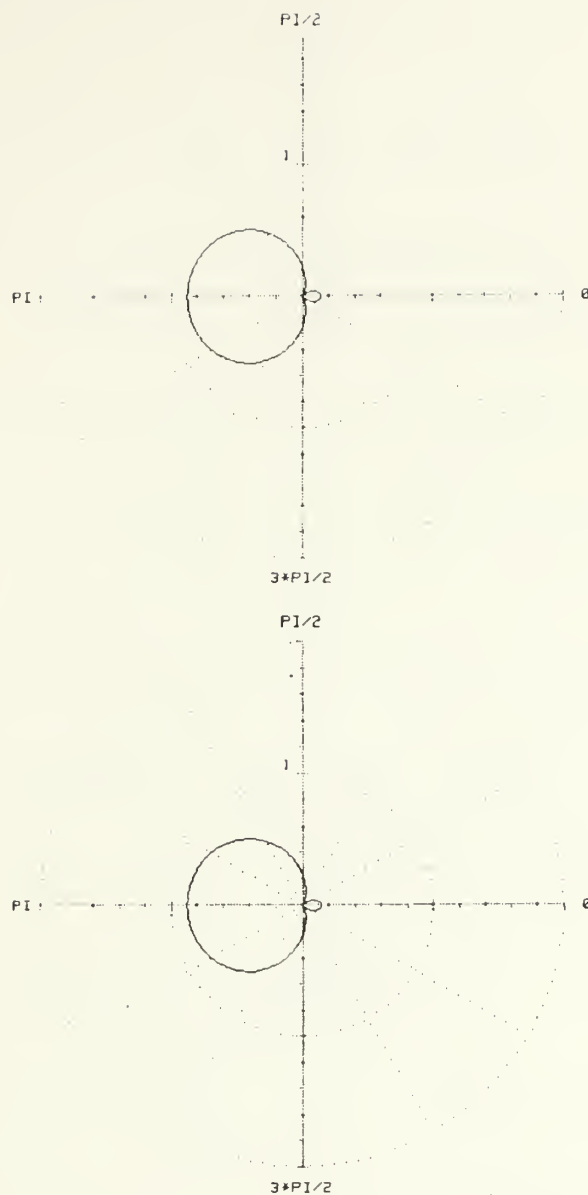
gives. It should be noted that the precision criteria of σ was greater than that normally encountered. [Ref's. 18, 19, 20 and 22]

The graphics subprograms of the differential scattering cross section program provided outputs for comparisons to Figure 80 in

Morse [Ref. 17] and Figure 10.10 of Bowman [Ref. 16]. These comparisons were used to verify the functioning and output of the differential scattering cross section program.

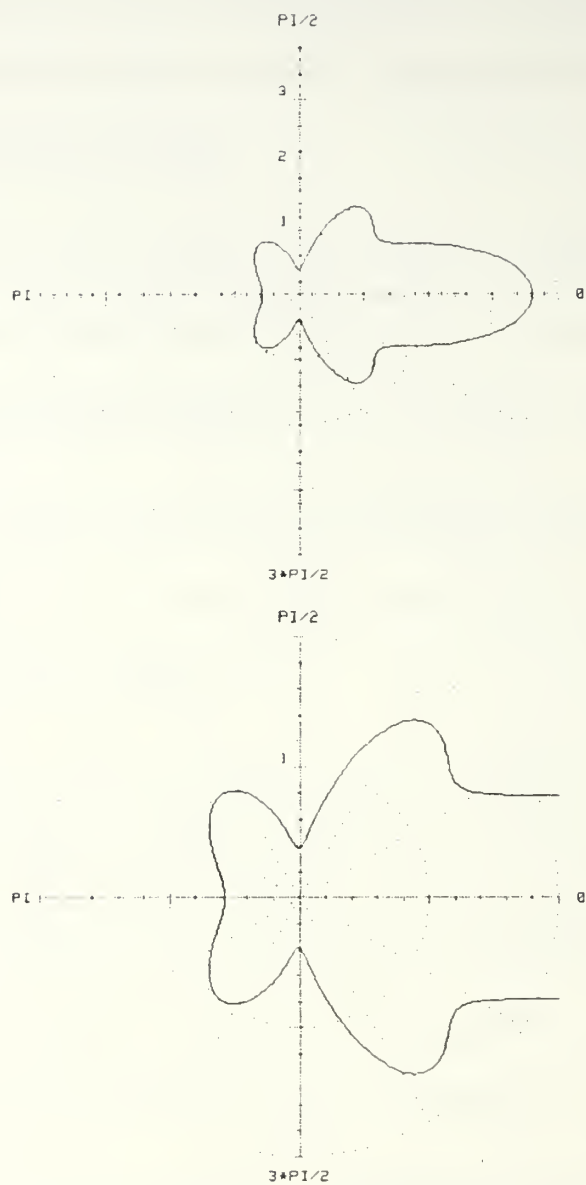
The graphics subprograms used to generate Figure 4 provide linear polar plots of the differential scattering cross section $\sigma(\Omega)$ normalized by the cross sectional area A_{tgt} of the target sphere. These linear polar plots show the normalized differential scattering cross section of acoustically hard spheres ensonified by plane acoustic waves incident from the left, i.e. from $\vartheta = \pi$.

The first view of each sheet in Figure 4 shows the entire normalized differential scattering cross section pattern, including the forward lobe, or "shadow zone", along $\vartheta = 0$. The second view of each sheet is a magnified plot showing the scattering detail at a scale comparable to the normalized backscattered cross section value. Note the two views are identical on Sheet 1. The need for magnification with increasing ka becomes apparent on subsequent sheets.



$C = 343 \text{ M/S.}$
 $F = 5000 \text{ HZ.}$
 $A = .0109180290961 \text{ M.}$
 $K \cdot A = 1.$
 $\text{NORMALIZED BCKSCTR} = .880073464081$

Figure 4, Sheet 1 of 3: Differential Scattering Cross Section Program Output for Comparison to Figure 80 of Morse [Ref. 17].



$C = 343 \text{ M/S.}$
 $F = 5000 \text{ HZ.}$
 $A = .0327540872883 \text{ M.}$
 $K \cdot A = 3 .$
 NORMALIZED BCKSCTR = .574927362173

Figure 4, Sheet 2 of 3: Differential Scattering Cross Section Program Output for Comparison to Figure 80 of Morse [Ref. 17].

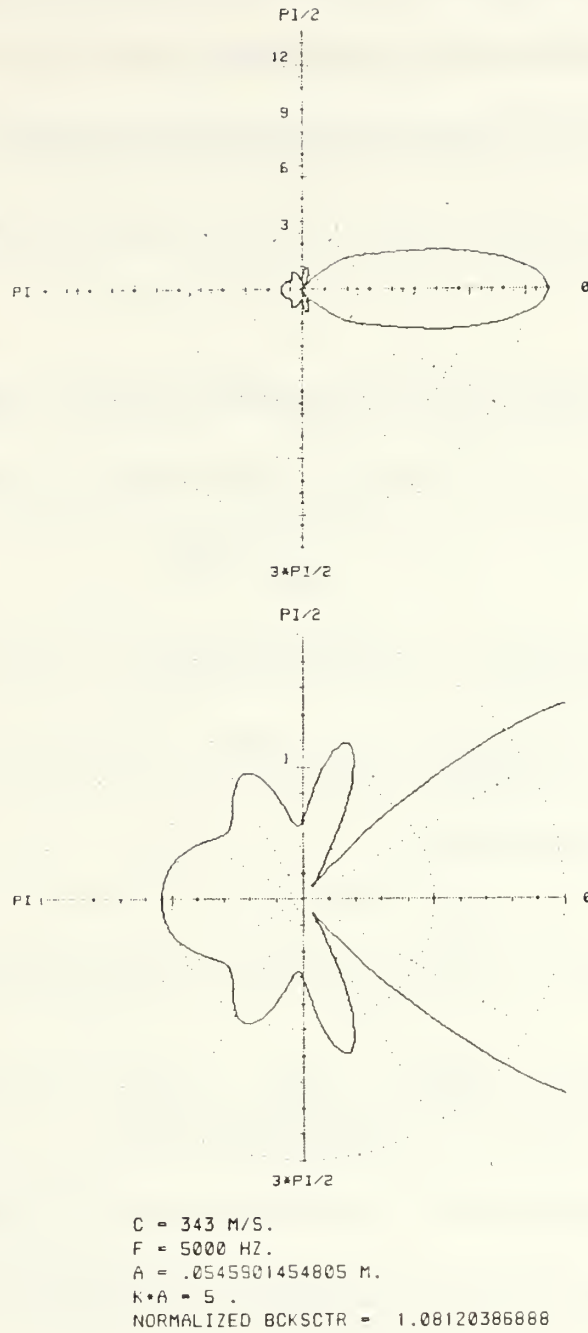


Figure 4, Sheet 3 of 3: Differential Scattering Cross Section Program Output for Comparison to Figure 80 of Morse [Ref. 17].

Figure 4 was used for comparison to Figure 80 of Morse [Ref. 17].

The radial scale of Morse was not graduated so verification consisted of a check for the correct number and approximate angular location of minimums and maximums in the differential scattering cross section patterns.

The graphics subprograms used to generate Figure 5 provide semi-logarithmic plots of the scattering modulus S of Bowman [Ref. 16].

$$S = k s(\theta) / \sqrt{4\pi} \quad (94)$$

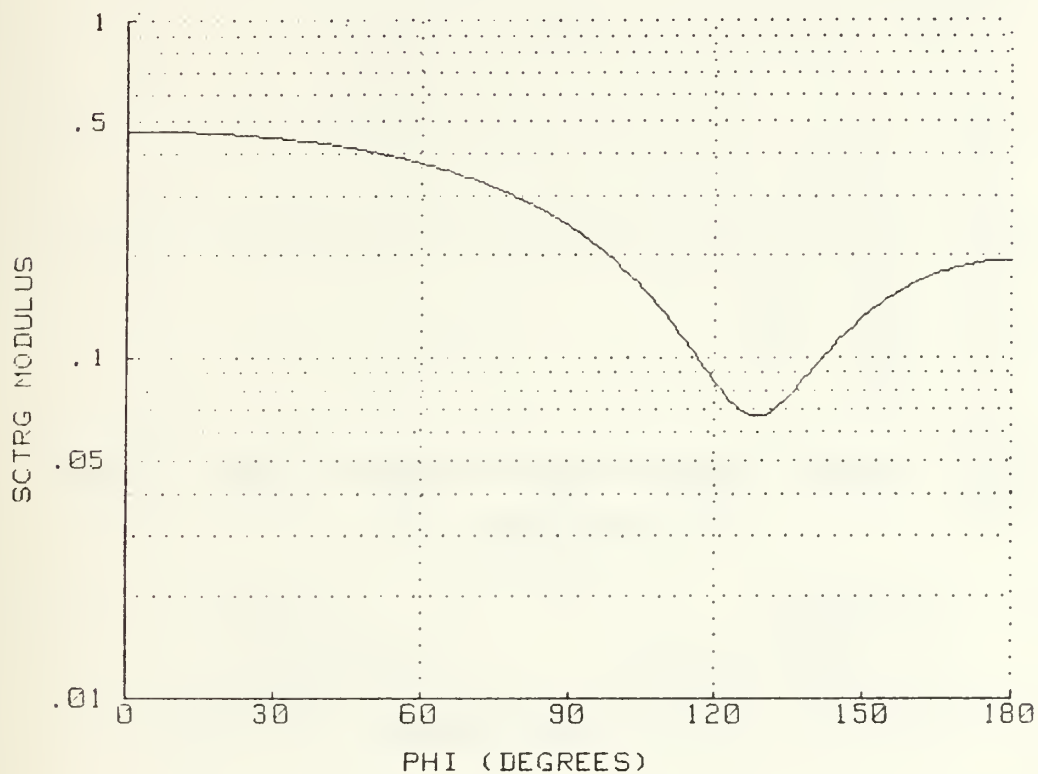
is the scattering modulus S of Bowman [Ref. 16]. $s(\theta)$ is the scattering amplitude $s(\Omega)$, as defined by equation (83), with a factor of $(-1)^l$ introduced into the sum, that is,

$$s(\theta) = \frac{\sqrt{4\pi}}{k} i \sum_{l=0}^{\infty} (-1)^l (2l+1) P_l(\cos \theta) a_l' \quad (95)$$

$s(\Omega)$ is normally used to calculate $\sigma(\Omega)$, per equation (84). The scattering modulus S of Bowman [Ref. 16] could also be used to calculate $\sigma(\Omega)$. Note the introduction of $(-1)^l$ into the summation corresponds to the case of an acoustically hard sphere ensonified by a plane acoustic wave incident from $\theta = 0$.

Comparison of Figure 5 to Figure 10.10 of Bowman [Ref. 16]

shows a match in both θ and S . This graphical match verifies the functioning and output of the differential scattering cross section program of Appendix B.



$C = 343 \text{ M/S.}$

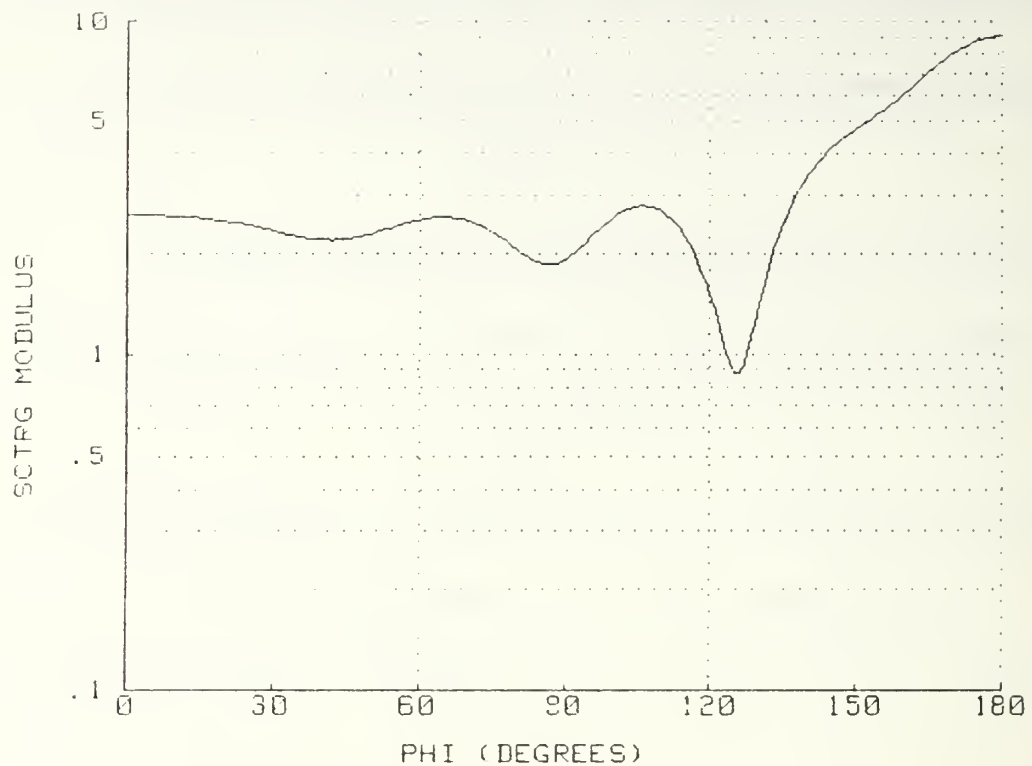
$F = 5000 \text{ HZ.}$

$A = .0109180290961 \text{ M.}$

$K \cdot A = 1 .$

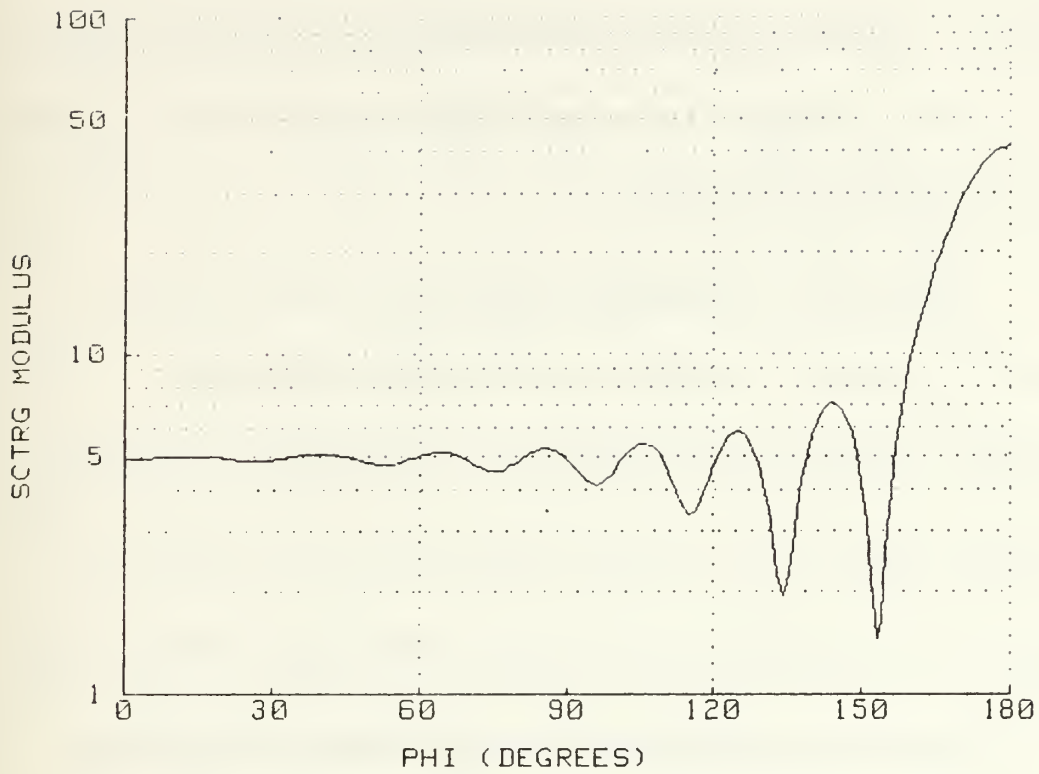
NORMALIZED BCKSCTR = .880073464081

Figure 5, Sheet 1 of 3: Differential Scattering Cross Section Program Output for Comparison to Figure 10.10 of Bowman [Ref. 16].



$C = 343 \text{ M/S.}$
 $F = 5000 \text{ HZ.}$
 $A = .0545901454805 \text{ M.}$
 $K \cdot A = 5 .$
 NORMALIZED BCKSCTR = 1.08120386888

Figure 5, Sheet 2 of 3: Differential Scattering Cross Section Program Output for Comparison to Figure 10.10 of Bowman [Ref. 16].



C = 343 M/S.

F = 5000 HZ.

A = .109180290961 M.

K*A = 10 .

NORMALIZED BCKSCTR = .957615718739

Figure 5, Sheet 3 of 3: Differential Scattering Cross Section Program Output for Comparison to Figure 10.10 of Bowman [Ref. 16].

2. Backscattered Cross Section Software Development

The differential scattering cross section program of Appendix B was modified to yield the backscattered cross section program of Appendix C. With the modification the normalized differential scattering cross section is calculated for the backscattered direction only. Equation (86b) is used for this calculation.

Additionally, the graphics subprograms of the differential scattering cross section program were replaced by one graphics subprogram. The new graphics subprogram was designed to provide a rectangular graph of the normalized backscattered cross section, σ_b . σ_b is plotted as a function of ka for a specifiable range of values of ka .

Figure 6 was generated by the backscattered cross section program. It was used for comparison to Figure 10.11 of Bowman [Ref. 16]. This comparison served as a verification of the calculated, normalized backscattered cross section values. Note the ka axis is labeled $K*A$.

Figure 7 was generated to verify the normalized backscattered cross section profile was approaching a value of one as ka left the Mie scattering regime and entered the "geometric optics" region. Note the ka axis is labeled $K*A$.

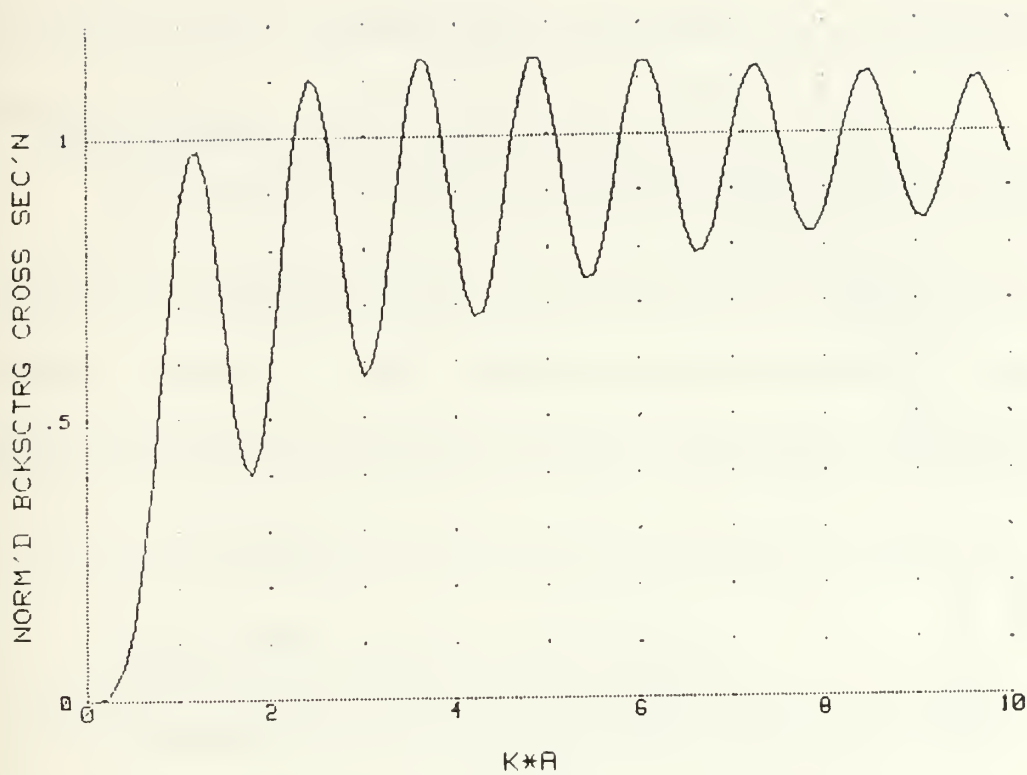


Figure 6: Backscattered Cross Section Program Output for Verification of Calculated Normalized Backscattered Cross Section Values by Comparison to Figure 10.11 of Bowman [Ref. 16].

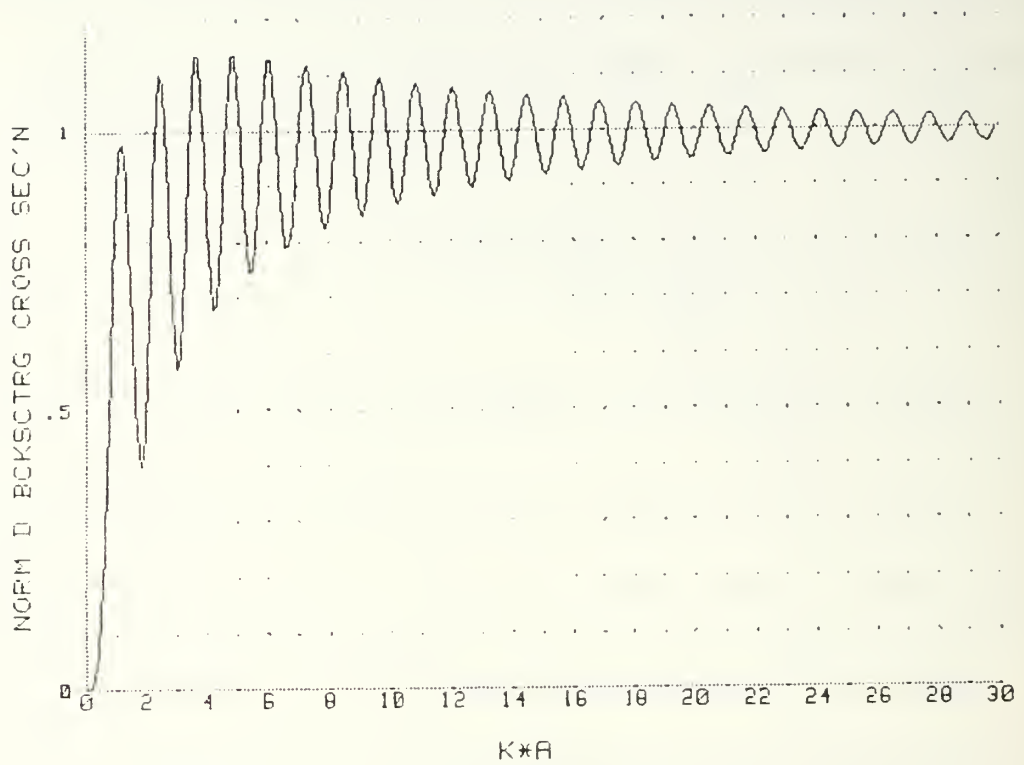


Figure 7: Backscattered Cross Section Program Output for Verification of the Normalized Backscattered Cross Section Asymptotic Behavior with Increasing ka .

3. Acoustic Array Efficiency Software Development

The acoustic array efficiency program in Appendix D determined $E_r E_t$. In general, each major section of Chapter II of this thesis and each set of analyzed data is represented by a subprogram of the acoustic array efficiency program.

The acoustic array efficiency program of Appendix D includes the non-graphics subprograms present in the backscattered cross section program of Appendix C. It also includes subprograms designed to furnish stored data, calculate attenuation and range using equations (27) through (42), and use developed information to calculate $E_t G_0$ with equation (17).

Equation (86b) was used to calculate σ_b .

The appropriate subprogram and main program calculational results were then used in equation (26) to determine E_r . E_r was used in equation (92) to determine $E_r E_t$.

B. DATA ACQUISITION AND SUPPORTING EQUIPMENT

Data collection occurred 28 November 1987, 30 November 1987, and 7 December 1987.

Data collected 28 November and 30 November provided information needed for calculation of $\sigma_b E_r E_t G_0$. Data collected 7 December allowed calculation of $E_t G_0$ and the calculation of E_r 's.

Collected data is presented in Appendix E.

1. Two Way Propagation Path Measurements

Two way propagation path data were collected 28 and 30 November. Measurements were used to calculate the product $\sigma_b E_r E_t G_0$.

Figure 8 provides a connection schematic for the data acquisition equipment.

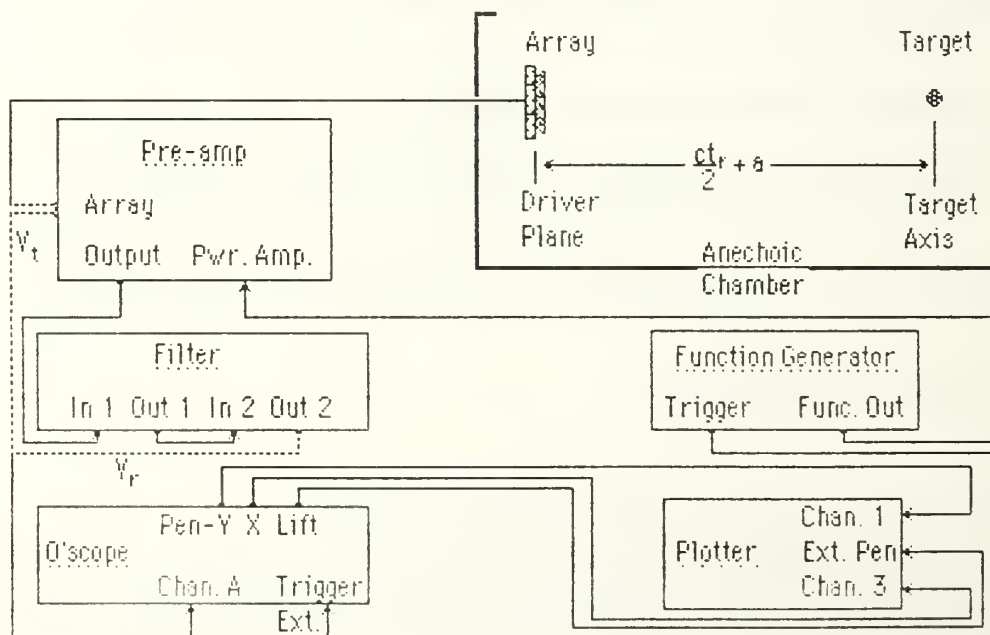


Figure 8: Data Acquisition Equipment Set-up

Four target spheres were available and measured for size. They included one hollow aluminum sphere (sphere number one) and three solid aluminum and brass spheres. Table (1) lists the data and the calculated values of $A_{tgt} = \pi a^2$, ka , and σ_b . σ_b was calculated from equation (86b).

Table 1: Target Sphere Dimensional Data and Normalized Backscattered Cross Section Computational Results for Frequency of 5000 [Hz].

Target No.	Sphere Diameter [m]	Sphere Radius [m]	A_{tgt} [m ²]	ka	σ_b
1	.2546 ±.0006	.1273	.05091	11.62	.9142
2	.1013 ±.0001	.05065	.008060	4.619	1.000
3	.07634±.00003	.03817	.004577	3.479	1.051
4	.06240±.00008	.03120	.003058	2.843	.6836

Figure 9 shows the target spheres' theoretical normalized backscattered cross section distribution plotted on a graph generated by the backscattered cross section program of Appendix C.

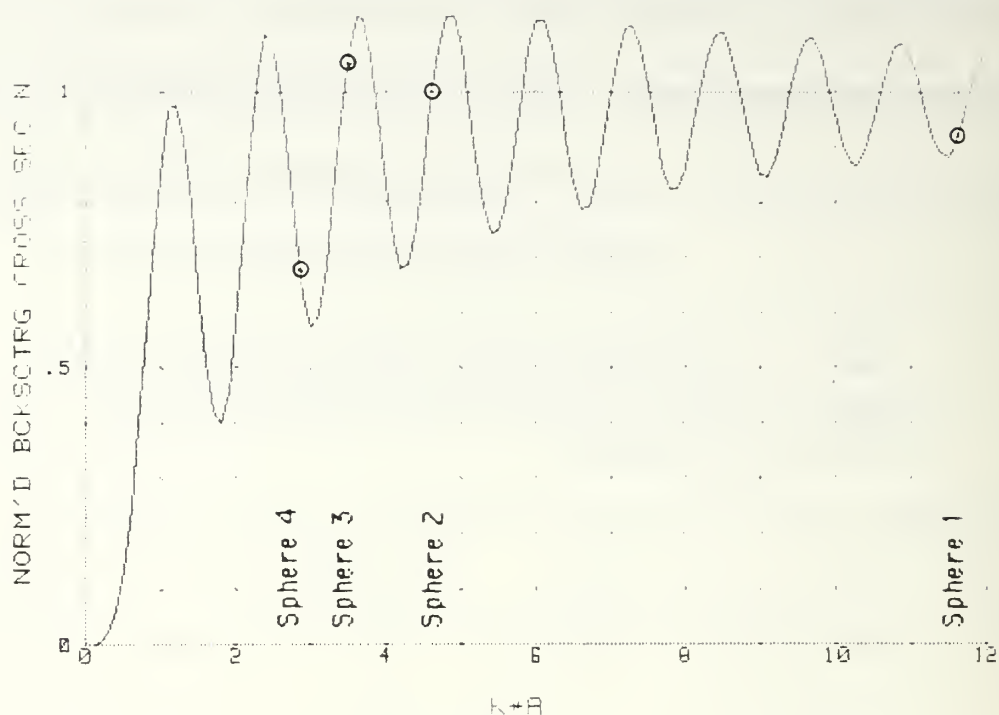


Figure 9: Target Spheres' Normalized Backscattered Cross Section Distribution as Calculated from Measured Diameters, Using an Assumption of Perfect Acoustic Hardness.

The target spheres were suspended in turn in the anechoic chamber. Placement was made using the criteria in Section D.1 of Chapter II. The range R from the array to a target was determined to be 5.30 [m].

Temperature T_c and relative humidity Rh along the propagation path were determined with a Weathermeasure Temperature and Relative

Humidity Meter. T_c was usually about 21 [°C] with a relative humidity of approximately 50%. Atmospheric pressure P was read from a barogram supplied by the Naval Postgraduate School meteorological station. Specific T_c , Rh , and P data are furnished in Appendix E.

The unshrouded, close packed, hexagonal acoustic array of Moxcey [Ref. 8] was used to ensonify each target.

$$A = N_s \pi r_s^2 \quad (96)$$

determined the aperture area A of the array. $N_s = 19$ was the number of speakers in the array and $r_s = .0381$ [m] was the average speaker horn radius [Ref. 8].

Moxcey [Ref. 8] determined the half width of the array's main lobe to be 12°. The angular half widths of targets two, three and four were all less than 5% of the main lobe's half width. Target one's angular half width was 11.5% of the main lobe's half width.

A sinusoidal input from a Hewlett Packard 3314 A function generator drove the array via a pre-amplifier. Signal input from the HP3314A function generator to the pre-amplifier was set for 20 cycles at 5000 [Hz]. The voltage input to the pre-amplifier's power amplifier

terminal (see Figure 8) was 3.5 [V] for spheres two, three and four and 3.0 [V] for sphere one.

Twenty cycles is considerably less than the number of cycles expected in actual echosounder application. It was necessary to keep the pulse packet this small because the anechoic chamber's corner was only about 1.5 [m] from the target mounting location. Voltage input for sphere one was reduced to 3.0 [V] to avoid clipping of its greater return signal voltage.

Actual transmission voltage inputs V_t to the array from the pre-amplifier were measured with a Nicolet 3091 oscilloscope at the pre-amplifier's array terminal. The array was disconnected from the pre-amplifier for V_t measurements. V_t values are provided in Appendix E. They are also stored in the Trans30 and Trans35 subprograms of the acoustic array efficiency program in Appendix D.

The Nicolet oscilloscope was connected to a Hewlett Packard 7090 A measurement plotting system. This connection provided a hard copy plot of voltage vs. time traces.

The returned signal was amplified and filtered. Pre-amplifier gain G_p was determined as 11,094 by Moxcey [Ref. 8].

Filtering was done with a Wavetek Brickwall filter model 753 A to remove the low frequency normal modes of oscillation of the speaker drivers from the return signal. Filtering was accomplished at 0 [dB] gain and 5000 [Hz] for both low and high pass settings.

The processed return signal voltages V_r were displayed and measured on the Nicolet 3091 oscilloscope. V_r measurements were made at the Out 2 terminal of the Wavetek Brickwall filter (see Figure 8). They were taken at 10 [μ S] intervals for two full cycles along the asymptotic region of the return signal trace.

The Nicolet 3091 oscilloscope was connected to the Hewlett Packard 7090 A measurement plotting system. Figure 10 shows the Hewlett Packard plotter's traces for target sphere two's return signal voltages as printed and subsequently labeled. The figure is representative of the oscilloscope traces for each target return. Data for all targets are provided in Appendix E.

The time of return t_r was determined as the time difference between the first positive maxima of the transmitted pulse packet and the first positive maxima of the target's return pulse packet.

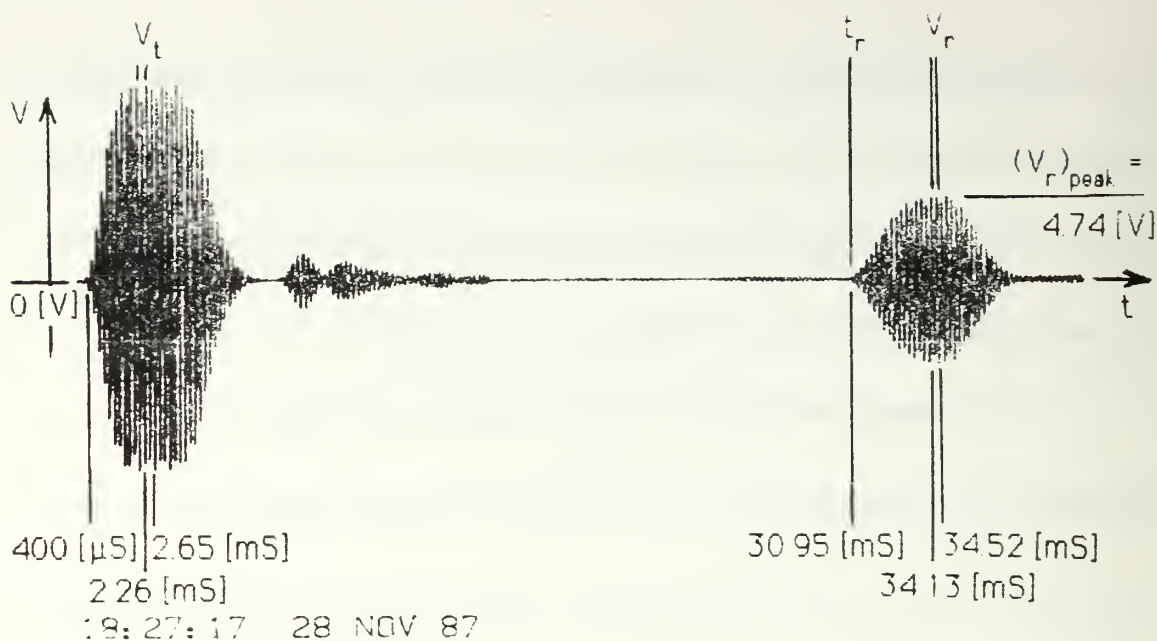
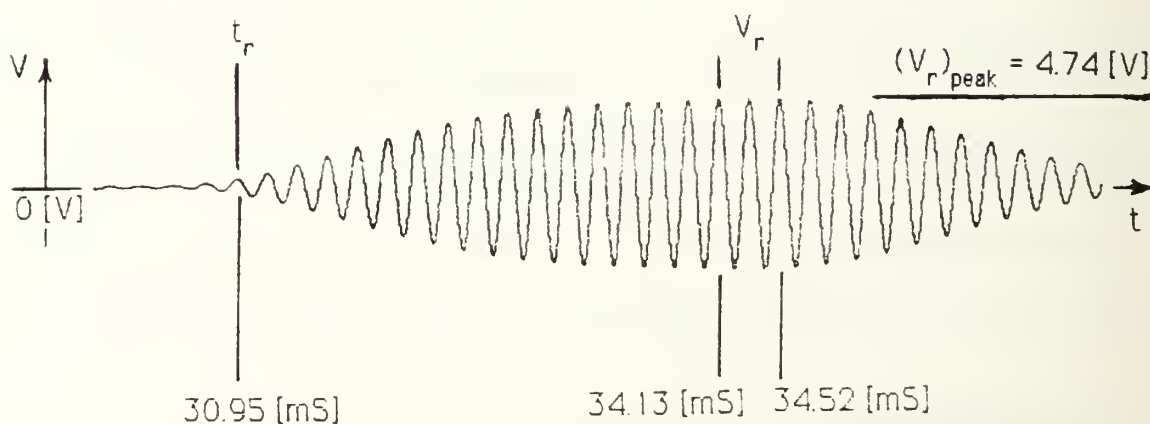


Figure 10, Sheet 1 of 2: Target Sphere Two's 5000 [Hz] Return Signal Trace



18:28:37 28 NOV 87

Figure 10, Sheet 2 of 2: Target Sphere Two's 5000 [Hz] Return Signal Trace, Scaled Down For Oscilloscope Measurement.

Noise voltage V_n measurements were made with the same measuring equipment setup used for V_r measurements. The target spheres were removed. V_n measurements were taken at a time of return t_r comparable to the time of measurement of V_r .

V_n measurements were actually made on occasions well separated chronologically from the V_r measurements. Therefore, they were proportionally corrected in line 2530 of the acoustic array efficiency program. The corrections account for the slight variations in input voltages and propagation path attenuations that occurred between the two measurement occasions.

Figure 11 shows a representative noise trace. Data from the noise measurements is presented in Appendix E and stored in the Noise30 and Noise35 subprograms of the acoustic array efficiency program in Appendix D.

Unless otherwise specified above the remaining data from the two way propagation path measurements are stored in the subprograms titled Sphere1, Sphere2, Sphere3 and Sphere4. All remaining data are also presented in Appendix E.

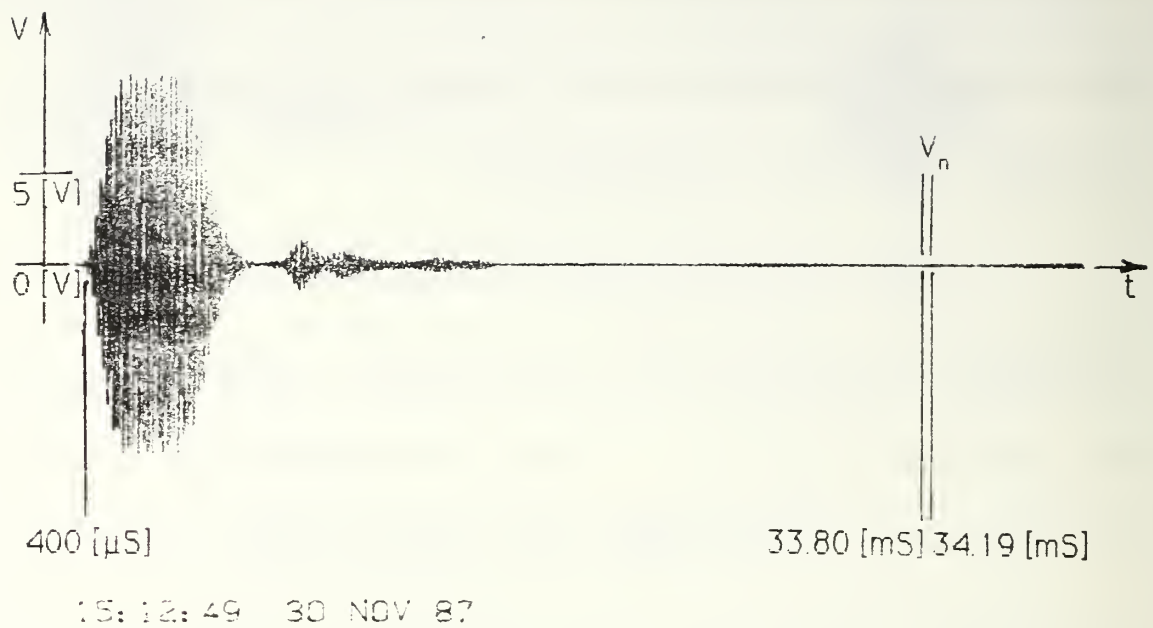


Figure 11: Representative 5000 [Hz] Noise Trace.
3.0 [V] Supplied by the HP3314A Function Generator.

2. One Way Propagation Path Measurements

One way propagation path data were collected 7 December. Measurements were used to calculate $E_t G_o$ with equation (17).

Data from the one way propagation path measurements are provided in Appendix E. Data are also stored in the Gain30 and Gain35 subprograms of the acoustic array efficiency program of Appendix D.

For one way path measurements, i.e. for the determination of $E_t G_0$, an Ivie Electronics Inc. IE 30 A Audio Analyzer (Serial #805 A 426) was used to measure received target intensity I_r in [dB]. Intensity measurements were referenced to 10^{-12} [W/m²]. The acoustic signal supplied for this measurement was a continuous wave at 5000 [Hz]. Measurements were taken at the suspension site of the calibrating targets.

A Fluke 8060 A True RMS Multimeter was used to measure the root-mean-square voltage $(V_{rms})_t$ supplied to the acoustic array at its input. $(V_{rms})_t$ was squared to determine $(V_{ms})_t$.

The Weathermeasure temperature and relative humidity meter was unavailable for $E_t G_0$ data collection. Hygrothermographs from the Naval Postgraduate School's meteorological station were used to estimate the anechoic chamber's relative humidity Rh and temperature T_c on 7 December. Estimates were based on comparisons to the hygrothermographs and measured Rh and T_c of 28 and 30 November.

C. RESULTS

Data analysis was performed with the aid of the acoustic array efficiency program of Appendix D. Data used in calculations is furnished in Appendix E.

The product $\sigma_b E_r E_t G_o$ was generated from two way propagation path data and application of equation (26). The average of calculated σ_b 's compared to the average of the experimental product $\sigma_b E_r E_t G_o$ gives a normalizing product $E_r E_t G_o$. The experimental product $\sigma_b E_r E_t G_o$ and the normalizing product $E_r E_t G_o$ are used to calculate experimental σ_b 's. These results are supplied in Table 2.

Table 2: Target Sphere Experimental, Normalized Backscattered Cross Section Computational Results.

Target No.	ka [m ²]	Calc'd σ_b	$\sigma_b E_r E_t G_o$	$E_r E_t G_o$	Exp'l σ_b
1	11.62	.9142	55.90		.947
2	4.619	1.000	59.88		1.01
3	3.479	1.051	61.62		1.04
4	2.843	.6836	37.98		.644
Avg.		.912	53.85	59.0	

The experimental σ_b are plotted on a graph generated by the backscattered cross section program of Appendix C. This plot is Figure 12. It is similar to Figure 9 and gives σ_b as a function of ka . Note ka is labeled $K*A$.

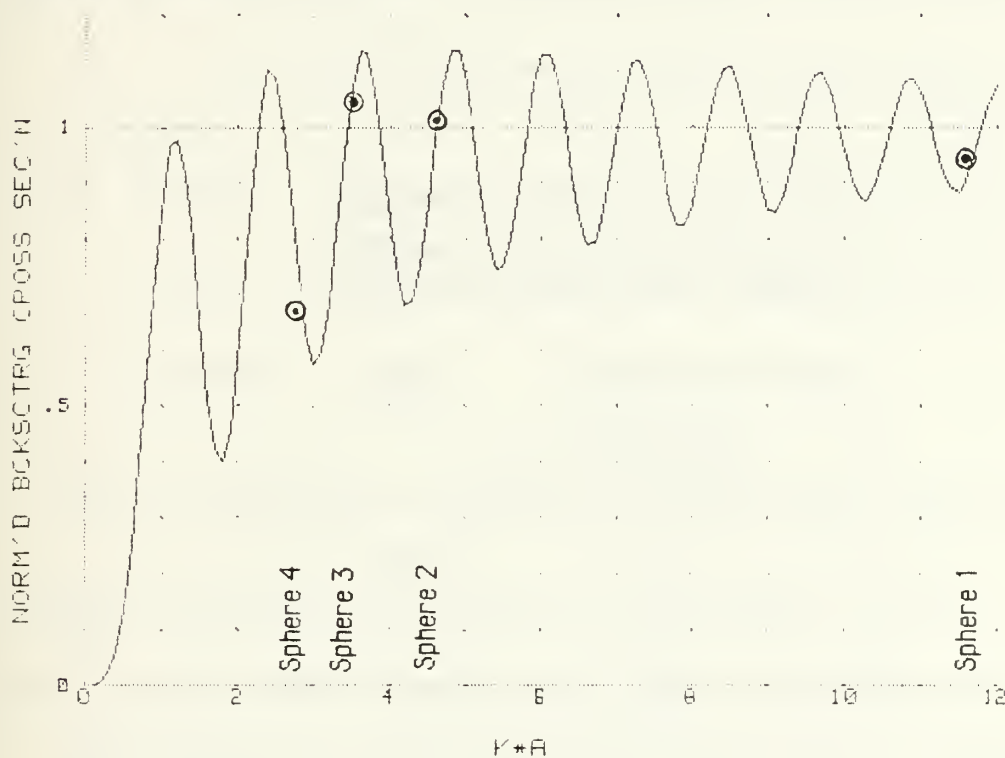


Figure 12: Target Spheres' Experimental, Normalized Backscattered Cross Section Distribution Compared to a Calculated Backscattered Cross Section Distribution Curve Generated by the Backscattered Cross Section Program of Appendix C.

As ka increases the experimental σ_b distribution rises from just below the calculated σ_b curve to just above it.

$E_t G_o$ was determined using one way propagation path data and equation (17). $E_t G_o$, or E_t , was assumed to be the same for spheres two, three, and four because the supply voltage and target locations were the same. The angular half widths of target spheres two, three and four were between 4.6% and 2.8% of the echosounder's main lobe's half width.

Table 3: Acoustic Array Product $E_t G_o$
Determined from One Way Propagation
Path Measurements and Equation (17).

Target No.	HP3314A Func'n Gen'r Supply Volt. [V]	$E_t G_o$
1	3.0	94.70
2	3.5	95.11
3	3.5	95.11
4	3.5	95.11

Calculated σ_b , $E_t G_o$ and two way propagation path data were used in equation (26) to determine E_r . σ_b values were calculated from the target

spheres' measured diameters, $2a$. A_{tgt} was calculated as πa^2 . Calculation results are furnished in Table 4.

Table 4: E_r and $E_t E_r$. E_r Determined From Two Way Propagation Path Data and Equation (26). $E_t E_r$ Determined From Assumption of Efficiency Reciprocity.

Target No.	$A_{tgt} [m^2]$	Calc'd σ_b	$\sigma_b A_{tgt} [m^2]$	E_r	$E_t E_r$
1	.05091	.9142	.04654	.6456	.4169
2	.008060	1.000	.008060	.6296	.3964
3	.004577	1.051	.004810	.6167	.3803
4	.003058	.6836	.002090	.5841	.3411

The E_r 's determined for Moxcey's unshrouded hexagonal array are in the range of .58 to .65. This is above the value range of 0.5 ± 0.1 determined by Weingartner for his square acoustic array [Ref. 6].

Table 4 results were used to construct Figures 13 and 14. Figure 13 gives E_r as a function of the calculated, normalized backscattered cross section, σ_b . Figure 14 gives E_r as a function of the apparent target size,

$\sigma_b A_{tgt}$.

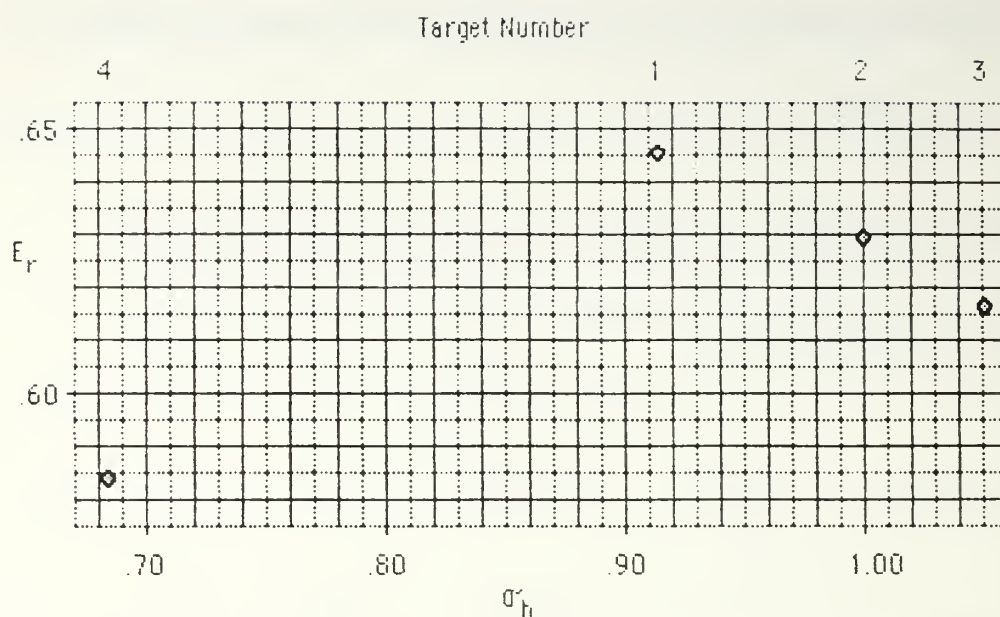


Figure 13: Acoustical to Electrical Power Conversion Efficiencies, E_r , as a Function of the Normalized Backscattered Cross Sections, σ_b , Calculated from Measured Sphere Sizes.

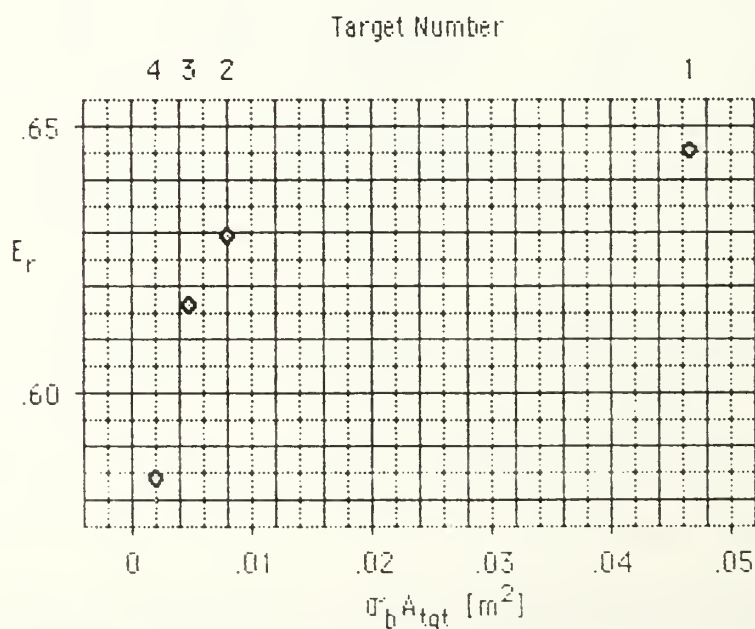


Figure 14: Acoustical to Electrical Power Conversion Efficiencies, E_r , as a Function of the Apparent Target Sizes, $\sigma_b A_{tgt}$.

Recalling equation (20),

$$P_{tgt} = \left[\frac{P_a}{4\pi} \right] \left[e^{-\alpha R} G(\Omega) \right] \left[\frac{A_{tgt}}{R^2} \right], \quad (20)$$

and equation (12),

$$P_{ra} = \frac{P_{tgt}}{4\pi R^2} \sigma_b e^{-\alpha R} A, \quad (12)$$

serves as a reminder that the received acoustic power, P_{ra} , depends on the apparent target size, $\sigma_b A_{tgt}$.

Figure 14's trend and the dependency of P_{ra} on $\sigma_b A_{tgt}$ were used as suggestions for the construction of Figure 15. Figure 15 is a plot of E_r

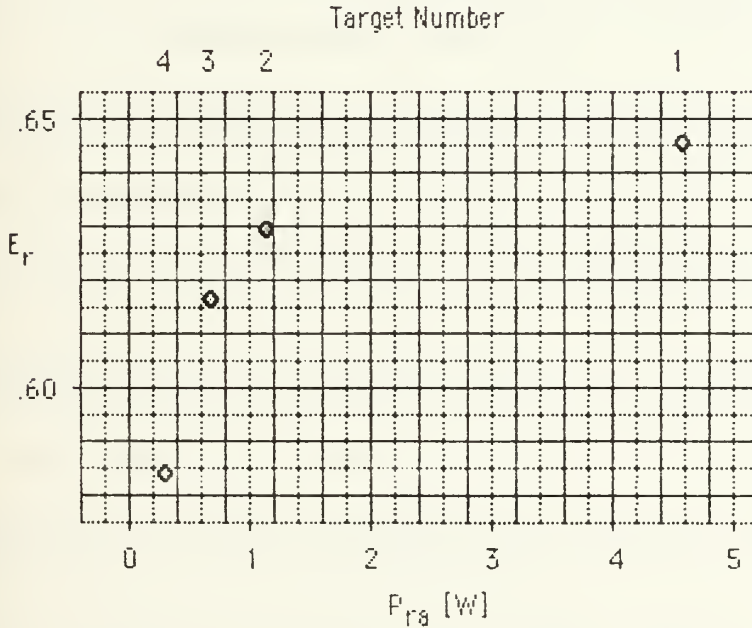


Figure 15: Acoustical to Electrical Power Conversion Efficiencies, E_r , as a Function of the Received Acoustic Powers, P_{ra} .

versus P_{ra} . P_{ra} was calculated using the definition (from equation (21))

$$P_{ra} = P_r / E_r \quad (97)$$

and the relationship (from equation (15))

$$P_r = (V_{ms})_r / Z \quad (98)$$

Note Figure 15's trend is for E_r to increase with an increase in P_{ra} for the range of target sizes investigated.

IV. CONCLUSIONS AND RECOMMENDATIONS

A. CONCLUSIONS

The larger magnitudes of E_r determined for Moxcey's hexagonal array suggest it may be more efficient than Weingartner's square array.

However, the drivers for each array are identical.

The 0.08 to 0.15 differences in efficiencies are more likely the result of the difference in calibration methods. Weingartner's measurements [Ref. 6] used steady state, continuous waves. The use of steady state, continuous waves allows the development of standing waves. This calibration investigation used pulsed waves. The use of pulsed waves did not provide sufficient time for standing waves to completely develop in the backscattered energy. [Ref. 26] This calibration method should provide more accurate efficiency values since it more nearly approximates the echosounder system's actual field operating configuration.

Additionally, steel braid and nylon lines were used to suspend the target spheres. These supports probably reflected enough acoustic energy to have a small influence on results. Other fixtures in the anechoic

chamber, such as support clamps and lights, may have also contributed small amounts of reflected energy to the returned signal.

Calibration of the computer controlled echosounder required determination of the product $E_r E_t$. The calibration process assumed $E_r = E_t$. The calibration results in Tables 3 and 4 for spheres two, three, and four indicate E_r varied with constant $E_t G_0$, or constant E_t . Such a variation negates the assumption of reciprocity for E_r and E_t .

Figure 15 suggests the acoustic array's efficiency E_r increased in response to an increase in P_{ra} and $(V_{rms})_r$.

The acoustic gain for spheres two, three and four was probably not constant, as assumed. However, G_0 is the maximum for $G(\Omega)$, and E_r is inversely proportional to G_0 , per equation (26). An averaging process accounting for the slight differences in gain encountered by spheres two, three and four would have increased the data points spread observed in Figures 14 and 15.

Additionally, the pre-amplifier's gain may not have been constant for the range of received voltage values encountered. This would have introduced either an apparent increase in E_r or dampened an increase in E_r .

with an increase in $(V_{rms})_r$. Such a gain variation could have effectively negated the assumption of efficiency reciprocity. However, this pre-amplifier is approximately 0.1% linear for less than 10 [V] peak [Ref. 26]. Received voltages in this investigation were all less than 10 [V].

B. RECOMMENDATIONS

Because efficiency reciprocity is now in question it is necessary to determine G_0 by calculation or measurement. Such a determination would allow the desired calibration quantity $E_r E_t$ to be written as

$$E_r E_t = E_r \frac{E_t G_0}{G_0} . \quad (99)$$

One method of calculating G_0 would involve integrating the acoustic array's calculated or measured intensity pattern (see Moxcey [Ref. 8]) for determination of an equivalent isotropic emitter. To determine G_0 the centroid intensity of the array's emitted intensity pattern would be compared to that of the equivalent isotropic emitter. This would be repeated for each transmission power level of interest.

Calculation of G_0 would allow a determination of E_t using $E_t G_0$. Such a determination of E_t would allow a reciprocity comparison to E_r and support a more accurate evaluation of $E_r E_t$.

The accuracy of E_r and $E_t G_0$ could be further refined as follows.

Use a calibrating site that allows the use of a pulse train closer in length to actual field use.

Make target return and noise voltages and site intensity measurements as chronologically close as possible.

Measure the barometric pressure in the propagation path directly along with the relative humidity and temperature.

The received and transmitted electrical powers for E_r and the transmitted electrical power for $E_t G_0$ were all measured at the pre-amplifier end of the pre-amplifier/array transmission line. This included transmission line power losses due to impedance as efficiency decreases. The present calibration process includes the transmission line impedance as part of the array impedance.

The amount this impedance power loss actually affects E_r could be evaluated by determining the impedances seen in each direction at the

pre-amplifier's array terminal. This would be an opportune time to verify the validity of transmission line impedance reciprocity.

Use the Nicolet oscilloscope to record a triggered readout from a calibrated microphone suspended at the target site at 45^0 to the centroid's axis. This would allow $E_t G_0$ to be determined for a pulse packet rather than for a continuous wave. Coupled with a proper calibrating site selection this technique should minimize interference problems such as anechoic chamber corner reflections.

A larger number of apparent target sizes spanning the desired range of apparent target sizes should be used to redetermine E_r for Moxcey's array. The E_r distribution should be examined for a smooth and asymptotic behavior. Comparative E_r values for Moxcey's array could be determined using the method outlined by Weingartner [Ref. 6].

Weingartner's square array's E_r could also be determined with this thesis' calibration process and compared to Weingartner's E_r value [Ref. 6].

The refined E_r curve in the now calibrated echosounder system should be used to develop an absolute C_T^2 plot of an air mass. An established method such as a tower mounted vertical array of thermocouples would be

used simultaneously to generate a comparative absolute C_T^2 plot of the same air mass.

C. SUMMARY

Realizing the potential of the computer controlled echosounder for analyzing lower atmospheric turbulence required a calibration of the echosounder. This thesis described theory and software for performing calculations crucial to a backscattered cross section calibration of the echosounder. The backscattered cross section calibration was evaluated in this thesis.

E_r 's values indicate the evaluated calibration process requires some refinement. They also indicate the calibration method possesses sufficient merit to warrant further development and that the software performs as intended.

APPENDIX A

ANECHOIC CHAMBER DESCRIPTION

The anechoic chamber is located in room 019 of building 232 at the Naval Postgraduate School. Acoustic research on sound sources, sound receivers and sound scatterers may be conducted in the chamber with a minimum of interference from wall reflection and external noise.

Wall reflection is minimized by 102 centimeter deep wedges made of P.F. 612 fiberglass. The wedges are attached to the walls, ceiling and floor of the chamber. Approximately 142 cubic meters of fiberglass is used to absorb 99% of incident sound energy for frequencies greater than 100 Hertz. External noise isolation is accomplished by separating the chamber's inner concrete block sides from the outer 12 inch concrete walls with a two inch thick lining of fiberglass and cork.

A usable region of approximately 8.2 meters by 4.3 meters by 3.4 meters is available. This region is floored by a grid of 225 wire cables, with each cable placed in a tension of 150 to 200 pounds per square inch. *

*This Appendix was compiled from the description posted by the entrance to the anechoic chamber instrumentation and control room.

APPENDIX B

DIFFERENTIAL SCATTERING CROSS SECTION PROGRAM

Examples of the output of this program are Figures 4 and 5, located in Chapter III.

```

10  !$$$$$$$$$$$$$$$$$$$$$$$$$$$$$$$$$$$$$$$$$$$$$$$$$$$$$$$$$$$$$$$
20  !
30  REM  ++++++
40  REM  ACOUSTICALLY HARD SPHERE SCATTERING OF PLANE ACOUSTIC WAVES
50  REM
60  REM  THIS PROGRAM CALCULATES AND GRAPHS THE DIFFERENTIAL SCATTERING
70  REM  CROSS SECTION AND/OR SCATTERING MODULUS FOR AN ACOUSTICALLY HARD
80  REM  SPHERE OF DIAMETER D ENSONIFIED BY AN INCIDENT PLANE WAVE OF
90  REM  FREQUENCY F.
100 REM
130 REM  ++++++
140 !
150 !++++ VARIABLE DECLARATIONS AND DEFINITIONS +++++
160 !
170 !
180 REAL C ! SPEED OF SOUND.
190 !
200 REAL Freq ! FREQUENCY OF THE EMITTER.
210 !
220 REAL A ! RADIUS OF THE SPHERE.
230 !
240 REAL L ! ORDER OF THE FUNCTION CALCULATED
250 ! IN A SUBROUTINE. IT IS USED
260 ! AS A LOOP INDEX AND TO DESIGNATE
270 ! THE ARRAY ELEMENT FOR THE FUNCTION
280 ! OF CORRESPONDING ORDER.
290 !
300 REAL Lmax ! MAX. SIGNIFICANT ORDER OF THE SUM
310 ! DETERMINING THE DIFFERENTIAL
320 ! SCATTERING CROSS SECTION (DSCS)
330 ! AND SCATTERING MODULUS (SM).
340 !
350 REAL K ! THE WAVE NUMBER,  $2 \cdot \pi \cdot \text{FREQ} / C$ .
360 !
370 REAL Ka !  $K \cdot A$ , THE ARGUMENT OF THE REGULAR
380 ! AND IRREGULAR SPHERICAL BESSEL
390 ! FUNCTIONS AND THEIR DERIVATIVES.
400 !

```

```

410 REAL J(51)          ! ARRAY FOR THE REGULAR SPHERICAL
420                      ! BESSEL FUNCTIONS (RSB) OF
430                      ! ARGUMENT KA AND ORDER 0 THROUGH
440                      ! LMAX.
450                      !
460 REAL Dj(51)         ! ARRAY FOR THE DERIVATIVES OF THE
470                      ! RSB (THE DRSB).
480                      !
490 REAL Y(51)          ! ARRAY FOR THE IRREGULAR SPHERICAL
500                      ! BESSEL FUNCTIONS (ISB) OF
510                      ! ARGUMENT KA AND ORDER 0 THROUGH
520                      ! LMAX.
530                      !
540 REAL Dy(51)         ! ARRAY FOR THE DERIVATIVES OF THE
550                      ! ISB (THE DISB).
560                      !
570 REAL P(51)          ! ARRAY FOR THE LEGENDRE
580                      ! POLYNOMIALS OF ARGUMENT COS(PHI).
590                      !
600 REAL Sm(360)        ! THE ARRAY REPRESENTING THE
610                      ! SCATTERING MODULUS (SM).
620                      !
630 REAL Ds(360)        ! THE ARRAY REPRESENTING THE
640                      ! DIFFERENTIAL SCATTERING CROSS
650                      ! SECTION NORMALIZED BY THE CROSS
660                      ! SECTIONAL AREA OF THE SPHERE
670                      ! (DSCS).
680                      ! NOTE DS(PHI)=4*SM(PHI)^2/KA^2.
690                      !
700                      ! ++++ NOTE ++++
710                      ! THE ARRAY DIMENSIONS (30+21) NEED
720                      ! TO BE INCREASED TO ACCOMODATE
730                      ! KA>30.
740                      !
750 !+++++
760 !
770 !++++ MAIN PROGRAM +++++
780                      !
790                      !
800 CALL Init(C,Freq,A,Lmax,Ka) ! INPUT AND CALCULATE REQUIRED
810                      ! PARAMETERS.
820                      !
830 CALL Difscnr(Lmax,Ka,Dj(*),J(*),Dy(*),Y(*),P(*),Sm(*),Ds(*))
840                      ! CALCULATE THE SM(*) AND DS(*).
850                      !
860 CALL Outprt(C,Freq,A,Ka,Sm(*),Ds(*)) ! OUTPUT THE SM(*) AND/OR DS(*).
870                      !
880                      !
890 !+++++
900 !

```

```

910  !++++ MAIN PROGRAM CONCLUSION +++++
920                                     !
930  PRINTER IS 1
940  PRINT
950  PRINT "END"                      ! ADVISES THE USER OF THE MAIN
960  PRINT                          ! PROGRAM'S CONCLUSION.
970  END
980                                     !
990  !++++
1000 !
1010 ! $$$$$$$$$$$$$$$$$$$$$$$$$$$$$$$$$$$$$$$$$$$$$$$$$$$$$$$$$$$$$
1020 !

```

```

1030 !
1040 !$$$$$$$$$$$$$$$$$$$$$$$$$$$$$$$$$$$$$$$$$$$$$$$$$$$$$$$$$$$$$$$$$$$$$$$$$$$
1050 SUB Init(C,Freq,A,Lmax,Ka)
1060 REM ++++++
1070 REM THIS MODULE REQUESTS THE APPROPRIATE INPUT VARIABLES TO DETERMINE
1080 REM C, FREQ, A, LMAX, AND KA.
1090 REM ++++++
1100 !
1110 !++++ MODULE VARIABLE DECLARATIONS AND DEFINITIONS +++++
1120 !
1130 !
1140 REAL Temp ! AMBIENT AIR TEMPERATURE IN DEG C.
1150 !
1160 REAL Circ ! CIRCUMFERENCE OF THE TGT. SPHERE.
1170 !
1180 REAL Diam ! DIAMETER OF THE TARGET SPHERE.
1190 !
1200 !
1210 !+++++
1220 !
1230 !+++ REQUESTING AND CALCULATING SYSTEM PARAMETERS ++++
1240 !
1250 !
1260 PRINTER IS 1 ! INPUTS ARE REQUESTED ON THE CRT.
1270 !
1280 Choice=0 ! *** DETERMINING C ***
1290 WHILE Choice<>1 AND Choice<>2
1300 PRINT
1310 PRINT "DO YOU DESIRE TO INPUT"
1320 PRINT " (1) THE SPEED OF ";
1330 PRINT "SOUND,"
1340 PRINT " OR (2) THE AMBIENT AIR ";
1350 PRINT "TEMPERATURE?"
1360 PRINT
1370 INPUT Choice
1380 END WHILE
1390 !
1400 IF Choice=1 THEN ! DIRECTLY ENTER C,
1410 PRINT "PLEASE ENTER C IN M/S."
1420 INPUT C
1430 END IF
1440 !
1450 IF Choice=2 THEN ! OR CALCULATE C FROM TEMP.
1460 PRINT "PLEASE ENTER TEMP IN ";
1470 PRINT "DEGREES CELSIUS."
1480 INPUT Temp
1490 Temp=Temp+273.15
1500 C=20.05*SQR(Temp)
1510 END IF
1520 ! *** DETERMINING FREQ ***
1530 PRINT ! DIRECTLY ENTER FREQ.
1540 PRINT "PLEASE ENTER THE ECHOSOUNDER";
1550 PRINT " FREQUENCY IN HZ."
1560 PRINT
1570 INPUT Freq

```

[illegible]

```

2090 !
2100 !$$$$$$$$$$$$$$$$$$$$$$$$$$$$$$$$$$$$$$$$$$$$$$$$$$$$$$$$$$$$$$$
2110 SUB Difscat(Lmax,Ka,Dj(*),J(*),Dy(*),Y(*),P(*),Sm(*),Ds(*))
2120 REM ++++++
2130 REM THIS MODULE CALCULATES THE ARRAYS SM(*) AND DS(*) REPRESENTING THE
2140 REM SCATTERING MODULUS AND THE DIFFERENTIAL SCATTERING CROSS SECTION
2150 REM NORMALIZED BY THE CROSS SECTIONAL AREA OF THE SPHERE, RESPECTIVELY.
2160 REM ++++++
2170 !
2180 !++++ MODULE VARIABLE DECLARATIONS AND DEFINITIONS +++++
2190 !
2200 !
2210 REAL Fac ! FACTOR COMMON TO RSM AND ISM.
2220 !
2230 REAL Rsm ! THE REAL COMPONENT OF THE
2240 ! SCATTERING MODULUS, SM.
2250 !
2260 REAL Ism ! THE IMAGINARY COMPONENT OF THE
2270 ! SM.
2280 !
2290 REAL Fact ! FACTOR COMMON TO SM(PHI) & DS(PHI).
2300 !
2310 REAL Phi ! THE (POLAR) ANGLE OFF THE AXIS
2320 ! OF PROPAGATION OF THE INCIDENT
2330 ! PLANE WAVE, WITH ORIGIN AT THE
2340 ! SPHERE CENTER. COS(PHI) IS THE
2350 ! ARGUMENT OF THE LEGENDRE
2360 ! POLYNOMIALS P(*) OF ORDER 0
2370 ! THROUGH LMAX.
2380 !
2390 !
2400 !+++++
2410 !
2420 !++++ CALCULATING THE SM AND DSCS ARRAYS +++++
2430 !
2440 !
2450 CALL Drsb(Lmax,Ka,Dj(*),J(*)) ! CALCULATE THE DERIVATIVES OF THE
2460 ! REGULAR SPHERICAL BESSEL FUNCTIONS
2470 ! OF ORDER 0 THROUGH LMAX.
2480 CALL Disb(Lmax,Ka,Dy(*),Y(*)) ! CALCULATE THE DERIVATIVES OF THE
2490 ! IRREGULAR SPHERICAL BESSEL FUNC'NS
2500 ! OF ORDER 0 THROUGH LMAX.
2510 FOR Phi=0 TO 360
2520 !
2530 CALL Leg(Lmax,Ka,Phi,P(*)) ! CALCULATE THE ARRAY P(*).
2540 !
2550 Rsm=0 ! CALCULATING THE REAL AND IMAGINARY
2560 Ism=0 ! COMPONENTS OF THE SM.
2570 FOR L=0 TO Lmax
2580 Fac=(Dj(L)*(2*L+1)*P(L))/(Dj(L)*Dj(L)+Dy(L)*Dy(L))
2590 Rsm=Rsm+(Fac*Dy(L))
2600 Ism=Ism+(Fac*Dj(L))
2610 NEXT L

```


[illegible]

[illegible]

80

```

3710                                ! * CALCULATE THE L "NAKED"      *
3720    FOR Ordcnt=1 TO L            ! * NUMR FACTORS OF J(0)/J(L). *
3730        Bnm=Bnm+Binc            ! INCREMENT BNM.
3740        IF Nflag=0 THEN          ! CHECK NUMR=0 FLAG NOT SET;
3750            Numr=Bnm-Numr        ! UPDATE NUMR IF NUMR<>0.
3760            IF Numr<>0 THEN
3770                Rl=Rl*Numr        ! UPDATE RL IF UPDATED NUMR<>0.
3780                Numr=1.0/Numr     ! PREPARE NUMR FOR NEXT EVOLUTION.
3790                                ! CHECK SCALING OF UPDATED RL.
3800                IF ABS(Rl)>10^250 THEN CALL Scale(Rl,Scexp)
3810            ELSE
3820                Nflag=1
3830            END IF
3840        ELSE                      ! IF NFLAG<>0 THE PREVIOUS STEPS ARE
3850            Nflag=0                ! DEFERRED FOR ONE INCREMENT OF BNM.
3860        END IF
3870    NEXT Ordcnt
3880                                ! * CALCULATE THE REMAINING NUMR *
3890                                ! * AND DENR TERMS OF J(0)/J(L). *
3900                                !     NOTE WHEN NUMR=DENR THEN
3910                                !     RL=J(0)/J(L).
3920    WHILE Numr<>Denr OR Nflag=1 OR Dflag=1
3930        Bnm=Bnm+Binc            ! INCREMENT BNM.
3940                                !
3950        IF Nflag=0 THEN          ! CHECK NUMR=0 FLAG NOT SET;
3960            Numr=Bnm-Numr        ! UPDATE NUMR IF NUMR<>0.
3970            IF Numr<>0 THEN
3980                Rl=Rl*Numr        ! UPDATE RL IF UPDATED NUMR<>0.
3990                Numr=1.0/Numr     ! PREPARE NUMR FOR NEXT EVOLUTION.
4000                                ! CHECK SCALING OF UPDATED RL.
4010                IF ABS(Rl)>10^250 THEN CALL Scale(Rl,Scexp)
4020            ELSE
4030                Nflag=1
4040            END IF
4050        ELSE                      ! IF NFLAG<>0 THE PREVIOUS STEPS ARE
4060            Nflag=0                ! DEFERRED FOR ONE INCREMENT OF BNM.
4070        END IF
4080                                !
4090        IF Dflag=0 THEN          ! CHECK DENR=0 FLAG NOT SET;
4100            Denr=Bnm-Denr        ! UPDATE DENR IF DENR<>0.
4110            IF Denr<>0 THEN
4120                Rl=Rl/Denr        ! UPDATE RL IF UPDATED DENR<>0.
4130                Denr=1.0/Denr     ! PREPARE DENR FOR NEXT EVOLUTION.
4140                                ! CHECK SCALING OF UPDATED RL.
4150                IF ABS(Rl)>10^250 THEN CALL Scale(Rl,Scexp)
4160            ELSE
4170                Dflag=1
4180            END IF
4190        ELSE                      ! IF DFLAG<>0 THE PREVIOUS STEPS ARE
4200            Dflag=0                ! DEFERRED FOR ONE INCREMENT OF BNM.
4210        END IF
4220                                !
4230    END WHILE
4240                                !

```

```

4250                                     !
4260      J(L)=J(0)/(R1*10^(Scexp))      ! *** J(L) DETERMINED. ***
4270                                     !
4280      NEXT L                         !
4290                                     !
4300                                     !
4310      !+++++
4320      !
4330      !+++ MODULE CONCLUSION +++++
4340                                     !
4350      SUBEND                         !
4360                                     !
4370      !+++++
4380      !
4390      !$$$$$$$$$$$$$$$$$$$$$$$$$$$$$$$$$$$$$$$$$$$$$$$$$$$$$$$$$$$$
4400      !

```

[illegible]

[illegible]


```

5660 !
5670 !$$$$$$$$$$$$$$$$$$$$$$$$$$$$$$$$$$$$$$$$$$$$$$$$$$$$$$$$$$$$$$$$$$$
5680 SUB Outpt(C,Freq,A,Ka,Sm(*),Ds(*))
5690 REM ++++++
5700 REM THIS MODULE CONTROLS THE OUTPUT OF THE CALCULATED DSCS AND SM IN
5710 REM GRAPHICAL PRESENTATIONS.
5720 REM ++++++
5730 !
5740 !+++ MODULE VARIABLE DECLARATIONS AND DEFINITIONS ++++
5750 !
5760 REAL Desire ! INTERACTIVE LOOP CONTROL.
5770 !
5780 REAL Rpt ! POLARPLT SCALING CONTROL; A
5790 ! REPETITION INDEX.
5800 !
5810 !+++++
5820 !
5830 !+++ DETERMINING THE DESIRED OUTPUT ++++
5840 !
5850 Desire=0
5860 WHILE Desire<>1 AND Desire<>2 AND Desire<>3
5870 PRINT "DO YOU DESIRE"
5880 PRINT " (1) A PLOT OF THE DSCS,"
5890 PRINT " (2) A PLOT OF THE SM,"
5900 PRINT " OR (3) BOTH?"
5910 INPUT Desire
5920 END WHILE
5930 PRINTER IS 701
5940 |
5950 WHILE Desire<4
5960 IF Desire=1 OR Desire=3 THEN
5970 FOR Rpt=1 TO 2
5980 CALL Polarplt(Ds(*),Rpt) ! PLOTTING THE DSCS.
5990 PRINT
6000 NEXT Rpt
6010 END IF
6020 |
6030 IF Desire=2 THEN
6040 CALL Recplt(Sm(*)) ! PLOTTING THE SM.
6050 PRINT
6060 END IF
6070 |
6080 PRINT " ", "C =" ; C ; "M/S." ! ECHO SIGNIFICANT CALCULATED VALUES
6090 PRINT " ", "F =" ; Freq ; "HZ." ! AND INPUT PARAMETERS.
6100 PRINT " ", "A =" ; A ; "M."
6110 PRINT " ", "K*A =" ; Ka ; "."
6120 PRINT " ", "NORMALIZED ";
6130 PRINT "BCKSCTR = " ; Ds(180)
6140 PRINT CHR$(12) ! PRINTER FORM FEED.
6150 |
6160 IF Desire=1 OR Desire=2 THEN Desire=4
6170 IF Desire=3 THEN Desire=2
6180 END WHILE
6190 |

```



```

6750 !
6760 !++++ GRAPH CONSTRUCTION AND LABELLING +++++
6770 !
6780 !
6790 Xgumax=100*MAX(1,RATIO)
6800 Ygumax=100*MAX(1,1/RATIO)
6810 Gumax=MIN(Xgumax,Ygumax)
6820 !
6830 CSIZE 3 ! ** LABELLING MAJOR RADIALS **
6840 LINE TYPE 1
6850 MOVE Gumax,Gumax/2
6860 LORG 8
6870 LABEL "0"
6880 MOVE Gumax/2,Gumax
6890 LORG 6
6900 LABEL "PI/2"
6910 MOVE 0,Gumax/2
6920 LORG 2
6930 LABEL "PI"
6940 MOVE Gumax/2,0
6950 LORG 4
6960 LABEL "3*PI/2"
6970 ! ** DEFINES THE TOTAL PLOTTING **
6980 VIEWPORT 5,Gumax-5,5,Gumax-5 ! ** AREA IN GRAPH UNITS. **
6990 !
7000 ! ** SCALING THE GRAPH TO **
7010 ! ** USER UNITS. **
7020 Dtmx=0 ! DETERMINING MAX. RADIUS VALUE
7030 IF Rpt=1 THEN ! REQ'D FOR THE PLOT.
7040     FOR I=0 TO 360
7050         IF Dtmx<Ds(I) THEN Dtmx=Ds(I)
7060     NEXT I
7070 END IF
7080 Endpt=INT(Dtmx+1)
7090 IF Endpt<2 THEN Endpt=2
7100 SHOW -Endpt,Endpt,-Endpt,Endpt ! ISOTROPICALLY SCALES THE GRAPH.
7110 !
7120 LINE TYPE 4 ! ** MAJOR RADIALS CONSTRUCTION **
7130 Ring=INT(Endpt/5+1)
7140 Tick=.2*Ring
7150 AXES Tick,Tick,0,0,5,5,2
7160 !
7170 LINE TYPE 3 ! ** RANGE RING CONSTRUCTION **
7180 DEG
7190 LORG 7
7200 FOR R=1 TO Endpt/Ring
7210     LINE TYPE 1
7220     MOVE 0,R*Ring
7230     LABEL R*Ring ! LABELLING THE RANGE.
7240     LINE TYPE 3
7250     FOR Angle=0 TO 360 ! DRAWING THE RING.
7260         PLOT R*Ring*COS(Angle),R*Ring*SIN(Angle)
7270     NEXT Angle
7280     PENUP
7290 NEXT R

```

[illegible]


```

7670      !
7680      !$$$$$$$$$$$$$$$$$$$$$$$$$$$$$$$$$$$$$$$$$$$$$$$$$$$$$$$$$$$$$$$$$$$
7690      SUB Recplt(Sm(*))
7700      REM      ++++++
7710      REM      THIS MODULE MAPS THE CALCULATED SCATTERING MODULUS ARRAY SM(*) ON
7720      REM      A SEMI-LOG PLOT.
7730      REM      ++++++
7740      !
7750      !+++ MODULE VARIABLE DECLARATIONS AND DEFINITIONS ++++
7760      !
7770      !
7780      REAL Xgumax      ! THE MAXIMUM ABSCISSA VALUE IN
7790      ! GRAPHICS DISPLAY UNITS.
7800      !
7810      REAL Ygumax      ! THE MAXIMUM ORDINATE VALUE IN
7820      ! GRAPHICS DISPLAY UNITS.
7830      !
7840      REAL Dtmx        ! THE MAX. VALUE OF THE ARRAY SM(*).
7850      !
7860      REAL Dtmin       ! THE MIN. VALUE OF THE ARRAY SM(*).
7870      !
7880      REAL Mxy         ! THE MAX. ORDINATE SCALE VALUE IN
7890      ! USER DEFINED UNITS.
7900      !
7910      REAL Mny         ! THE MIN. ORDINATE SCALE VALUE IN
7920      ! USER DEFINED UNITS.
7930      !
7940      !
7950      !+++++
7960      !
7970      !+++ INITIALIZING THE PLOTTER ++++
7980      !
7990      GINIT
8000      PLOTTER IS CRT,"INTERNAL"
8010      GRAPHICS ON
8020      GCLEAR
8030      !
8040      !+++++
8050      !
8060      !+++ GRAPH CONSTRUCTION AND LABELLING ++++
8070      !
8080      !
8090      Xgumax=100*MAX(1,RATIO)
8100      Ygumax=100*MAX(1,1/RATIO)
8110      !
8120      CSIZE 4
8130      !
8140      LORG 4          ! ** LABELLING THE ABSCISSA AXIS **
8150      MOVE Xgumax/2,0
8160      LABEL "PHI (DEGREES)"

```

```

8170
8180 DEG
8190 LDIR 90
8200 LORG 6
8210 MOVE 0,Ygumax/2
8220 LABEL "SCTRG MODULUS"
8230 LDIR 0
8240
8250 VIEWPORT 15,Xgumax-5,10,Ygumax-5
8260
8270
8280 Dtmx=0
8290 Dtmn=Sm(180)
8300 FOR I=0 TO 180
8310     IF Dtmx<Sm(I) THEN Dtmx=Sm(I)
8320     IF Dtmn>Sm(I) THEN Dtmn=Sm(I)
8330 NEXT I
8340 Mxy=INT(LGT(Dtmx))+1
8350 Mny=INT(LGT(Dtmn))
8360
8370 WINDOW 0,180,Mny,Mxy
8380
8390 AXES 30,1,0,Mny,1,1,1.5
8400
8410 LINE TYPE 3
8420 FOR I=Mny TO Mxy
8430     FOR J=1 TO 9
8440         MOVE 0,I+LGT(J)
8450         PLOT 180,I+LGT(J),-1
8460         PENUP
8470     NEXT J
8480 NEXT I
8490
8500 FOR I=60 TO 180 STEP 60
8510     MOVE I,Mny
8520     PLOT I,Mxy,-1
8530     PENUP
8540 NEXT I
8550
8560 CLIP OFF
8570 LINE TYPE 1
8580
8590 LORG 6
8600 FOR I=0 TO 180 STEP 30
8610     MOVE I,Mny
8620     LABEL I
8630 NEXT I
8640
8650 LORG 8
8660 FOR I=Mny TO Mxy
8670     MOVE 0,I
8680     LABEL 10^I
8690     MOVE 0,I+LGT(5)
8700     LABEL (10^(I+1))/2
8710 NEXT I

```

! ** LABELLING THE ORDINATE AXIS **

! ** GRAPH CONSTRUCTION **

! DEFINES THE TOTAL PLOTTING AREA

! IN GRAPH UNITS.

! ** ORDINATE USER UNITS **

! ** DETERMINED. **

! ANISOTROPICALLY SCALES THE GRAPH

! TO USER UNITS.

! PLOTS THE AXES.

! * PLOTS THE HORIZONTAL *
! * LOGARITHMIC GRID LINES I.A.W. *
! * THE VERTICAL SCALE. *

! * PLOTS THE VERTICAL GRID LINES *
! * I.A.W. THE HORIZONTAL SCALE. *

! ** LABELLING THE ABSCISSA SCALE **

! ** LABELLING THE ORDINATE SCALE **

! POWER OF 10 LABELS.

! HALF THE NEXT POWER OF 10 LABELS.

APPENDIX C

BACKSCATTERED CROSS SECTION PROGRAM

Examples of the output of this program are Figures 6 and 7, located in Chapter III.

[illegible]

[illegible]

[illegible]

[illegible]

```

2420                                ! * CALCULATE THE L "NAKED" *
2430    FOR Ordcnt=1 TO L            ! * NUMR FACTORS OF J(0)/J(L). *
2440        Bnm=Bnm+Binc            ! INCREMENT BNM.
2450        IF Nflag=0 THEN          ! CHECK NUMR=0 FLAG NOT SET;
2460            Numr=Bnm-Numr        ! UPDATE NUMR IF NUMR<>0.
2470            IF Numr<>0 THEN
2480                Rl=Rl*Numr        ! UPDATE RL IF UPDATED NUMR<>0.
2490                Numr=1.0/Numr     ! PREPARE NUMR FOR NEXT EVOLUTION.
2500                                ! CHECK SCALING OF UPDATED RL.
2510                IF ABS(Rl)>10^250 THEN CALL Scale(Rl,Scexp)
2520            ELSE
2530                Nflag=1
2540            END IF
2550        ELSE                      ! IF NFLAG<>0 THE PREVIOUS STEPS ARE
2560            Nflag=0                ! DEFERRED FOR ONE INCREMENT OF BNM.
2570        END IF
2580    NEXT Ordcnt
2590                                ! * CALCULATE THE REMAINING NUMR *
2600                                ! * AND DENR TERMS OF J(0)/J(L). *
2610                                ! NOTE WHEN NUMR=DENR THEN
2620                                ! RL=J(0)/J(L).
2630    WHILE Numr<>Denr OR Nflag=1 OR Dflag=1
2640        Bnm=Bnm+Binc            ! INCREMENT BNM.
2650                                !
2660        IF Nflag=0 THEN            ! CHECK NUMR=0 FLAG NOT SET;
2670            Numr=Bnm-Numr        ! UPDATE NUMR IF NUMR<>0.
2680            IF Numr<>0 THEN
2690                Rl=Rl*Numr        ! UPDATE RL IF UPDATED NUMR<>0.
2700                Numr=1.0/Numr     ! PREPARE NUMR FOR NEXT EVOLUTION.
2710                                ! CHECK SCALING OF UPDATED RL.
2720                IF ABS(Rl)>10^250 THEN CALL Scale(Rl,Scexp)
2730            ELSE
2740                Nflag=1
2750            END IF
2760        ELSE                      ! IF NFLAG<>0 THE PREVIOUS STEPS ARE
2770            Nflag=0                ! DEFERRED FOR ONE INCREMENT OF BNM.
2780        END IF
2790                                !
2800        IF Dflag=0 THEN            ! CHECK DENR=0 FLAG NOT SET;
2810            Denr=Bnm-Denr        ! UPDATE DENR IF DENR<>0.
2820            IF Denr<>0 THEN
2830                Rl=Rl/Denr        ! UPDATE RL IF UPDATED DENR<>0.
2840                Denr=1.0/Denr     ! PREPARE DENR FOR NEXT EVOLUTION.
2850                                ! CHECK SCALING OF UPDATED RL.
2860                IF ABS(Rl)>10^250 THEN CALL Scale(Rl,Scexp)
2870            ELSE
2880                Dflag=1
2890            END IF
2900        ELSE                      ! IF DFLAG<>0 THE PREVIOUS STEPS ARE
2910            Dflag=0                ! DEFERRED FOR ONE INCREMENT OF BNM.
2920        END IF
2930                                !
2940    END WHILE

```

[illegible]

[illegible]

[illegible]

[illegible]

APPENDIX D

ACOUSTIC ARRAY EFFICIENCY PROGRAM

This program was used to analyze data and determine the calibration product $E_r E_t$. The output of this program was also used to construct Figures 13, 14, and 15.

The power supply mentioned in the Gain30 and Gain35 subprograms was the HP3314A function generator. All data contained in the data subprograms are repeated in Appendix E. Data units are available in Appendix E with their respective data.

```

10      !$$$$$$$$$$$$$$$$$$$$$$$$$$$$$$$$$$$$$$$$$$$$$$$$$$$$$$$$$$$$$$$
20      !
30      REM      ++++++
40      REM              ACOUSTIC ARRAY EFFICIENCY
50      REM
60      REM          THIS PROGRAM CALCULATES THE EFFICIENCY AND CENTERLINE GAIN OF
70      REM          AN ACOUSTIC ARRAY BASED ON THE RETURN FROM AN ACOUSTICALLY HARD
80      REM          SPHERE OF DIAMETER D ENSONIFIED BY AN INCIDENT PLANE WAVE OF
90      REM          FREQUENCY F.
100     REM
130     REM      ++++++
140     !
150     !+++ VARIABLE DECLARATIONS AND DEFINITIONS ++++++
160                                     !
170                                     !
180     REAL Vmsn                      ! MEAN SQUARE VOLTAGE RECEIVED FROM
190                                     ! THE TARGET SPHERE AND MEASURED
200                                     ! AFTER PRE-AMPLIFICATION.
210                                     !
220     REAL Vmsn                      ! MEAN SQUARE VOLTAGE RECEIVED IN
230                                     ! THE ABSCENCE OF A TARGET AND
240                                     ! MEASURED AFTER PRE-AMP.
250                                     !

```

260	REAL Vmst	! MEAN SQUARE VOLTAGE TRANSMITTED.
270		!
280	REAL R	! THE RANGE FROM THE PLANE OF THE
290		! ARRAY SPEAKER DIAPHRAGMS TO THE
300		! CENTER OF THE TARGET SPHERE AND TO
310		! THE SPECTRUM ANALYZER MICROPHONE.
320		!
330	REAL Et	! THE EFFICIENCY OF CONVERSION
340		! FROM TRANSMITTED ELECTRICAL POWER
350		! TO TRANSMITTED ACOUSTICAL POWER.
360		!
370	REAL Go	! THE CENTERLINE GAIN OF THE ACOUSTIC
380		! ARRAY.
390		!
400	REAL Etgo	! $ET \cdot GO$
410		!
420	REAL At	! THE ATTENUATION COEFFICIENT,
430		! "ALPHA".
440		!
450	REAL C,Cmoist	! THE SPEED OF SOUND IN HUMID AIR.
460		!
470	REAL Efreq	! THE SELECTED FREQUENCY OF THE
480		! ACOUSTIC ARRAY.
490		!
500	REAL K	! THE WAVE NUMBER, $2 \cdot \pi \cdot EFREQ/C$.
510		!
520	REAL A	! THE RADIUS OF THE TARGET SPHERE.
530		!
540	REAL Ka	! $K \cdot A$, THE ARGUMENT OF THE REGULAR
550		! AND IRREGULAR SPHERICAL BESSEL
560		! FUNCTIONS AND THEIR DERIVATIVES.
570		!
580	REAL Aa	! THE APERTURE AREA OF THE ARRAY.
590		!
600	REAL Gpre	! THE PRE-AMP'S ELECTRICAL GAIN.
610		!
620	REAL Nbs	! THE VARIABLE REPRESENTING THE
630		! NORMALIZED, BACKSCATTERED CROSS
640		! SECTION (NBCS).
650		!
660	REAL Atgt	! CROSS SECTIONAL AREA OF THE
670		! TARGET SPHERE.
680		!
690	REAL Sasph	! SURFACE AREA OF AN IMAGINARY
700		! SPHERE CENTERED ON THE ARRAY
710		! AND HAVING A RADIUS EQUAL TO
720		! THE RANGE TO THE CENTER OF THE
730		! TARGET SPHERE.
740		!
750	REAL Prat	! THE RATIO OF RECEIVED TARGET
760		! ELECTRICAL POWER TO THE
770		! TRANSMITTED ELECTRICAL POWER.
780		!

112


```

1790 REAL Patmn                ! Patm FOR NOISE DETERMINATION.
1800                            !
1810 REAL Efreqn              ! Efreqn=Efreq.
1820                            !
1830 REAL Cn                  ! C FOR NOISE DETERMINATION.
1840                            !
1850 REAL Atn                 ! At FOR NOISE DETERMINATION.
1860                            !
1870 REAL Vmstn              ! Vmst FOR NOISE DETERMINATION.
1880                            !
1890 REAL Rspkr              ! THE AVERAGE RADIUS OF AN ARRAY
1900                            ! SPEAKER.
1910                            !
1920                            !
1930 !+++++
1940 !
1950 !++++ DETERMINING SYSTEM PARAMETERS +++++
1960                            !
1970                            !
1980 PRINTER IS 1
1990 PRINT "WHICH TARGET DATA SET ";
2000 PRINT "DO YOU WISH ANALYZED?"
2010 PRINTER IS 701
2020 INPUT Sphere
2030 PRINT "TARGET NO. " ; Sphere
2040 PRINT
2050                            !
2060 IF Sphere=1 THEN
2070     Ch=3.0
2080     CALL Gain0(Ch,Etgo)
2090     CALL Sphere1(Vr(*),J,Tc,Patm,Rh,Tgttm,Dia,Efreq,Nuspr,Diaspr,Gpre)
2100     CALL Trans30(Jt,Vt(*))
2110     CALL Noise30(Jn,Jtn,Noise(*),Tnoise(*),Tcn,Rhn,Patmn,Efreqn)
2120 END IF
2130                            !
2140 IF Sphere=2 THEN
2150     Ch=3.5
2160     CALL Gain0(Ch,Etgo)
2170     CALL Sphere2(Vr(*),J,Tc,Patm,Rh,Tgttm,Dia,Efreq,Nuspr,Diaspr,Gpre)
2180     CALL Trans35(Jt,Vt(*))
2190     CALL Noise35(Jn,Jtn,Noise(*),Tnoise(*),Tcn,Rhn,Patmn,Efreqn)
2200 END IF
2210                            !
2220 IF Sphere=3 THEN
2230     Ch=3.5
2240     CALL Gain0(Ch,Etgo)
2250     CALL Sphere3(Vr(*),J,Tc,Patm,Rh,Tgttm,Dia,Efreq,Nuspr,Diaspr,Gpre)
2260     CALL Trans35(Jt,Vt(*))
2270     CALL Noise35(Jn,Jtn,Noise(*),Tnoise(*),Tcn,Rhn,Patmn,Efreqn)
2280 END IF
2290                            !

```


[illegible]


```

3930      !
3940      ! $$$$$$$$$$$$$$$$$$$$$$$$$$$$$$$$$$$$$$$$$$$$$$$$$$$$$$$$$$$$$$$$
3950 SUB Atten(Tc,Rh,Patm,Cmoist,At,Efreq)
3960 REM      ++++++
3970 REM      THIS MODULE CALCULATES THE ATTENUATION USING RELATIVE HUMIDITY
3980 REM      IN PERCENT, ATMOSPHERIC PRESSURE IN MILLIBARS, AND TEMPERATURE
3990 REM      IN DEGREES CENTIGRADE.
4000 REM      ++++++
4010      !
4020      ! ++++ MODULE VARIABLE DECLARATIONS AND DEFINITIONS ++++++
4030
4040
4050 REAL Tk              ! THE AMBIENT TEMPERATURE IN DEG. K.
4060
4070 REAL Es             ! THE SATURATION VAPOR PRESSURE.
4080
4090 REAL Pratio         ! THE RATIO OF WATER PRESSURE IN
4100                      ! MILLIBARS TO ATMOSPHERIC PRESSURE
4110                      ! IN MILLIBARS.
4120
4130 REAL Cdry           ! THE SPEED OF SOUND IN DRY AIR.
4140
4150 REAL H               !
4160
4170 REAL Past          ! P ASTERISK.
4180
4190 REAL Tast          ! T ASTERISK.
4200
4210 REAL Fm            ! MAX. FREQ.
4220
4230 REAL Amax          ! MAX EXPECTED ATTENUATION.
4240
4250 REAL Frat          ! EFREQ/FM
4260
4270 REAL F2            ! FRAT*FRAT
4280
4290 REAL Ac1,Amol       ! ATTENUATION EXPONENT COMPONENTS.
4300
4310
4320      ! ++++++
4330      !
```

[illegible]

[illegible]

[illegible]


```

6390                                ! *** CALCULATING THE RATIO ***
6400  FOR L=1 TO Lmax                ! *** J(0)/J(L). ***
6410      R1=1.0                    ! INITIALIZING RL.
6420      Numr=0.                   ! INITIALIZING NUMR.
6430      Denr=0.                   ! INITIALIZING DENR.
6440      Scexp=0.                  ! INITIALIZING SCEXP.
6450      Nflag=0.                  ! INITIALIZING NFLAG.
6460      Dflag=0.                  ! INITIALIZING DFLAG.
6470      Bnm=1.0/Ka                ! INITIALIZING BNM.
6480      Binc=2.0/Ka              ! CALCULATE BINC.
6490                                !
6500                                ! * CALCULATE THE L "NAKED" *
6510  FOR Ordcnt=1 TO L            ! * NUMR FACTORS OF J(0)/J(L). *
6520      Bnm=Bnm+Binc              ! INCREMENT BNM.
6530      IF Nflag=0 THEN           ! CHECK NUMR=0 FLAG NOT SET;
6540          Numr=Bnm-Numr          ! UPDATE NUMR IF NUMR<>0.
6550          IF Numr<>0 THEN
6560              R1=R1*Numr          ! UPDATE RL IF UPDATED NUMR<>0.
6570              Numr=1.0/Numr       ! PREPARE NUMR FOR NEXT EVOLUTION.
6580                                ! CHECK SCALING OF UPDATED RL.
6590              IF ABS(R1)>10^250 THEN CALL Scale(R1,Scexp)
6600          ELSE
6610              Nflag=1
6620          END IF
6630      ELSE                       ! IF NFLAG<>0 THE PREVIOUS STEPS ARE
6640          Nflag=0                 ! DEFERRED FOR ONE INCREMENT OF BNM.
6650      END IF
6660  NEXT Ordcnt
6670                                ! * CALCULATE THE REMAINING NUMR *
6680                                ! * AND DENR TERMS OF J(0)/J(L). *
6690                                ! NOTE WHEN NUMR=DENR THEN
6700                                ! RL=J(0)/J(L).
6710  WHILE Numr<>Denr OR Nflag=1 OR Dflag=1
6720      Bnm=Bnm+Binc              ! INCREMENT BNM.
6730                                !
6740      IF Nflag=0 THEN           ! CHECK NUMR=0 FLAG NOT SET;
6750          Numr=Bnm-Numr          ! UPDATE NUMR IF NUMR<>0.
6760          IF Numr<>0 THEN
6770              R1=R1*Numr          ! UPDATE RL IF UPDATED NUMR<>0.
6780              Numr=1.0/Numr       ! PREPARE NUMR FOR NEXT EVOLUTION.
6790                                ! CHECK SCALING OF UPDATED RL.
6800              IF ABS(R1)>10^250 THEN CALL Scale(R1,Scexp)
6810          ELSE
6820              Nflag=1
6830          END IF
6840      ELSE                       ! IF NFLAG<>0 THE PREVIOUS STEPS ARE
6850          Nflag=0                 ! DEFERRED FOR ONE INCREMENT OF BNM.
6860      END IF
6870                                !
6880      IF Dflag=0 THEN           ! CHECK DENR=0 FLAG NOT SET;
6890          Denr=Bnm-Denr          ! UPDATE DENR IF DENR<>0.
6900          IF Denr<>0 THEN
6910              R1=R1/Denr          ! UPDATE RL IF UPDATED DENR<>0.
6920              Denr=1.0/Denr       ! PREPARE DENR FOR NEXT EVOLUTION.

```


[illegible]

[illegible]

[illegible]

[illegible]

[illegible]

[illegible]

[illegible]

[illegible]

[illegible]

APPENDIX E

ACOUSTIC ARRAY CALIBRATION DATA

This appendix contains data used to determine the calibration product $E_r E_t$. Data units are contained in square brackets.

For listings of the same type of data the units and uncertainty are explicitly given for the first datum. Remaining data in the listing have the same units and uncertainty as the first datum.

1. TWO WAY PROPAGATION PATH DATA

Pre-amplifier gain G_g and array impedance Z were previously determined by Moxcey. G_g was determined to be 11,094. Z was determined to be 15.8 [Ω]. [Ref. 8]

The remaining data are presented in the following tables.

V_{supply} is the voltage supplied by the HP3314A function generator to the pre-amplifier (see Figure 8).

Table 5a: Two Way Propagation Path Data for Sphere One,
Collected 30 November 1987; Run #2: Data Re-measured
Because First Run V_r (with 3.5 [V] Supply) Was Clipped.

$$\text{Diameter} = 2a = .2546 \pm 0.0006 \text{ [m]}$$

$$T_c = 20.2 \pm 0.1 \text{ [}^\circ\text{C]}$$

$$Rh = 52.8 \pm 0.1 \text{ [%]}$$

$$P = 1016.8 \pm 0.2 \text{ [mb]}$$

$$\text{No. pulses} = 20$$

$$V_{\text{supply}} = 3.0 \text{ [V]}$$

$$t_r = 30.31 \text{ [mS]} - 400 \text{ [\mu S]} = 29.91 \pm 0.1 \text{ [mS]}$$

t	V_t	t	V_t
2.25 \pm 0.01[mS]	690 \pm 5 [mV]	2.45	690
2.26	680	2.46	680
2.27	590	2.47	590
2.28	440	2.48	430
2.29	320	2.49	320
2.30	160	2.50	150
2.31	- 20	2.51	- 40
2.32	-230	2.52	-240
2.33	-410	2.53	-420
2.34	-550	2.54	-560
2.35	-610	2.55	-620
2.36	-610	2.56	-600
2.37	-520	2.57	-510
2.38	-360	2.58	-380
2.39	-240	2.59	-240
2.40	- 80	2.60	- 70
2.41	110	2.61	120
2.42	320	2.62	330
2.43	490	2.63	500
2.44	630	2.64	640

Table 5b: Two Way Propagation Path Data for Sphere One Continued,
 Collected 30 November 1987; Run #2: Data Re-measured
 Because First Run V_r (with 3.5 [V] Supply) Was Clipped.

t	V_r	t	V_r
33.68 \pm 0.01[mS]	9.54 \pm 0.03 [V]	33.88	9.60
33.69	9.40	33.89	9.38
33.70	8.32	33.90	8.22
33.71	6.42	33.91	6.26
33.72	3.88	33.92	3.67
33.73	0.960	33.93	0.730
33.74	-2.07	33.94	-2.30
33.75	-4.90	33.95	-5.11
33.76	-7.24	33.96	-7.40
33.77	-8.87	33.97	-8.96
33.78	-9.64	33.98	-9.64
33.79	-9.45	33.99	-9.39
33.80	-8.32	34.00	-8.20
33.81	-6.41	34.01	-6.21
33.82	-3.83	34.02	-3.61
33.83	-0.890	34.03	-0.650
33.84	2.14	34.04	2.36
33.85	4.94	34.05	5.12
33.86	7.26	34.06	7.38
33.87	8.88	34.07	8.91

Table 6a: Two Way Propagation Path Data for Sphere Two,
Collected 28 November 1987.

Diameter = $2a = 10.13 \pm 0.01$ [cm]
 $T_c = 21.0 \pm 0.1$ [$^{\circ}$ C]
 $R_h = 49.8 \pm 0.1$ [%]
 $P = 1009.4 \pm 0.2$ [mb]
 No. pulses = 20
 $V_{\text{supply}} = 3.5$ [V]
 $t_r = 30.95$ [mS] - 400 [μ S] = 30.55 ± 0.1 [mS]

t	V_t	t	V_t
2.26 ± 0.01 [mS]	830 ± 5 [mV]	2.46	830
2.27	770	2.47	770
2.28	640	2.48	630
2.29	490	2.49	470
2.30	290	2.50	290
2.31	80	2.51	60
2.32	-180	2.52	-190
2.33	-400	2.53	-420
2.34	-610	2.54	-600
2.35	-730	2.55	-720
2.36	-770	2.56	-770
2.37	-720	2.57	-710
2.38	-580	2.58	-570
2.39	-430	2.59	-420
2.40	-240	2.60	-230
2.41	- 20	2.61	- 10
2.42	240	2.62	240
2.43	460	2.63	480
2.44	660	2.64	670
2.45	780	2.65	790

Table 6b: Two Way Propagation Path Data for Sphere Two Continued,
Collected 28 November 1987.

t	V _r	t	V _r
34.13 ±0.01[mS]	4.72 ± 0.01 [V]	34.33	4.74
34.14	4.66	34.34	4.66
34.15	4.16	34.35	4.13
34.16	3.23	34.36	3.19
34.17	2.01	34.37	1.95
34.18	0.560	34.38	0.500
34.19	-0.940	34.39	-1.00
34.20	-2.35	34.40	-2.40
34.21	-3.52	34.41	-3.57
34.22	-4.36	34.42	-4.38
34.23	-4.77	34.43	-4.78
34.24	-4.70	34.44	-4.68
34.25	-4.18	34.45	-4.15
34.26	-3.25	34.46	-3.20
34.27	-1.99	34.47	-1.92
34.28	-0.560	34.48	-0.480
34.29	0.960	34.49	1.02
34.30	2.34	34.50	2.39
34.31	3.51	34.51	3.54
34.32	4.34	34.52	4.34

Table 7: Two Way Propagation Path Data for Sphere Three,
Collected 28 November 1987.

Diameter = $2a = 7.634 \pm 0.003$ [cm]

$T_c = 21.3 \pm 0.1$ [$^{\circ}$ C]

Rh = 49.8 ± 0.1 [%]

P = 1009.6 ± 0.2 [mb]

No. pulses = 20

$V_{\text{supply}} = 3.5$ [V]

$t_r = 30.99$ [mS] - 400 [μ S] = 30.59 ± 0.1 [mS]

V_t data is the same as sphere two's (see Table 6a).

t	V_r	t	V_r
33.98 ± 0.01 [mS]	3.61 ± 0.03 [V]	34.18	3.63
33.99	3.40	34.19	3.39
34.00	2.86	34.20	2.84
34.01	2.04	34.21	2.02
34.02	1.01	34.22	0.970
34.03	-0.120	34.23	-0.180
34.04	-1.25	34.24	-1.30
34.05	-2.25	34.25	-2.31
34.06	-3.04	34.26	-3.08
34.07	-3.54	34.27	-3.56
34.08	-3.68	34.28	-3.69
34.09	-3.46	34.29	-3.46
34.10	-2.91	34.30	-2.89
34.11	-2.07	34.31	-2.04
34.12	-1.04	34.32	-0.990
34.13	0.110	34.33	0.160
34.14	1.25	34.34	1.29
34.15	2.24	34.35	2.26
34.16	3.00	34.36	3.05
34.17	3.48	34.37	3.50

Table 8: Two Way Propagation Path Data for Sphere Four,
Collected 28 November 1987.

Diameter = $2a = 6.240 \pm 0.008$ [cm]

$T_c = 21.4 \pm 0.1$ [$^{\circ}$ c]

Rh = 49.6 ± 0.1 [%]

P = 1009.9 ± 0.2 [mb]

No. pulses = 20

$V_{\text{supply}} = 3.5$ [V]

$t_r = 31.04$ [mS] - 400 [μ S] = 30.64 ± 0.1 [mS]

V_t data is the same as sphere two's (see Table 6a).

t	V_r	t	V_r
33.83 ± 0.01 [mS]	2.28 ± 0.03 [V]	34.03	2.29
33.84	2.10	34.04	2.10
33.85	1.68	34.05	1.68
33.86	1.10	34.06	1.09
33.87	0.420	34.07	0.400
33.88	-0.320	34.08	-0.340
33.89	-1.03	34.09	-1.04
33.90	-1.64	34.10	-1.66
33.91	-2.07	34.11	-2.10
33.92	-2.31	34.12	-2.32
33.93	-2.34	34.13	-2.35
33.94	-2.12	34.14	-2.12
33.95	-1.71	34.15	-1.70
33.96	-1.12	34.16	-1.11
33.97	-0.440	34.17	-0.400
33.98	0.320	34.18	0.340
33.99	1.02	34.19	1.04
34.00	1.62	34.20	1.64
34.01	2.06	34.21	2.08
34.02	2.28	34.22	2.28

Table 9: Noise Data for 3.0 [V] Supply Voltage;
Collected 30 November 1987.

$T_c = 20.8 \pm 0.1$ [$^{\circ}$ c] $R_h = 51.7 \pm 0.1$ [%] $P = 1016.7 \pm 0.2$ [mb]

$V_{\text{supply}} = 3.0$ [V] No. pulses = 20

V_t data is the same as sphere one's (see Table 5a).

t	V_n	t	V_n
33.73 \pm 0.01 [mS]	00 \pm 5 [mV]	34.03	-120
33.74	00	34.04	-120
33.75	- 20	34.05	-110
33.76	- 30	34.06	- 80
33.77	- 40	34.07	- 70
33.78	- 60	34.08	- 40
33.79	- 80	34.09	- 30
33.80	-100	34.10	- 20
33.81	-110	34.11	00
33.82	-120	34.12	00
33.83	-120	34.13	10
33.84	-110	34.14	00
33.85	-100	34.15	00
33.86	- 80	34.16	- 30
33.87	- 70	34.17	- 40
33.88	- 50	34.18	- 70
33.89	- 40	34.19	- 90
33.90	- 10	34.20	-110
33.91	00	34.21	-120
33.92	00	34.22	-120
33.93	00	34.23	-120
33.94	00	34.24	-120
33.95	- 20	34.25	-110
33.96	- 30	34.26	- 80
33.97	- 50	34.27	- 70
33.98	- 70	34.28	- 40
33.99	- 80	34.29	- 30
34.00	-100	34.30	00
34.01	-110	34.31	00
34.02	-120	34.32	10

Table 10a: Noise Data for 3.5 [V] Supply Voltage;
Collected 30 November 1987.

$$T_c = 21.3 \pm 0.1 [^{\circ} \text{C}]$$

$$Rh = 51.3 \pm 0.1 [\%]$$

$$P = 1016.6 \pm 0.2 [\text{mb}]$$

$$\text{No. pulses} = 20$$

$$V_{\text{supply}} = 3.5 [\text{V}]$$

t	V_t	t	V_t
2.24 ± 0.01 [mS]	740 ± 5 [mV]	2.44	750
2.25	830	2.45	830
2.26	820	2.46	810
2.27	720	2.47	700
2.28	530	2.48	500
2.29	380	2.49	360
2.30	180	2.50	160
2.31	- 60	2.51	- 80
2.32	-310	2.52	-330
2.33	-530	2.53	-540
2.34	-680	2.54	-690
2.35	-770	2.55	-760
2.36	-750	2.56	-740
2.37	-640	2.57	-630
2.38	-460	2.58	-460
2.39	-300	2.59	-280
2.40	-100	2.60	- 80
2.41	140	2.61	160
2.42	400	2.62	410
2.43	600	2.63	620

Table 10b: Noise Data for 3.5 [V] Supply Voltage Continued;
Collected 30 November 1987.

t	V _n	t	V _n
33.80 ± 0.01 [mS]	- 60 ± 5 [mV]	34.00	- 70
33.81	- 80	34.01	- 80
33.82	- 80	34.02	- 90
33.83	- 80	34.03	- 80
33.84	- 70	34.04	- 80
33.85	- 60	34.05	- 60
33.86	- 40	34.06	- 40
33.87	- 20	34.07	- 20
33.88	00	34.08	10
33.89	20	34.09	30
33.90	50	34.10	40
33.91	60	34.11	70
33.92	60	34.12	60
33.93	60	34.13	70
33.94	40	34.14	50
33.95	30	34.15	40
33.96	20	34.16	10
33.97	00	34.17	- 10
33.98	- 30	34.18	- 40
33.99	- 50	34.19	- 60

2. ONE WAY PROPAGATION PATH DATA

One way propagation path data are presented in the following tables.

T_c and Rh are estimated. The estimates were based on hygrothermographic comparisons and 28 and 30 November data.

Table 11: One Way Propagation Path Data for 3.0 [V], 5000 [Hz] Continuous Wave Supply from the HP3314A Function Generator; Collected 7 December 1987.

$$(V_{rms})_t = 0.246 \pm 0.001 \text{ [V]}$$

$$T_c \approx 21.0 \text{ [}^\circ\text{C]}$$

$$Rh \approx 50.0 \text{ [%]}$$

$$P = 1021.5 \pm 0.2 \text{ [mb]}$$

$$R = 5.30 \text{ [m]} \text{ (calculated from two way propagation path data for spheres two, three and four)}$$

$$I_r \text{ (referenced to } 10^{-12} \text{ [W/m}^2\text{])}$$

$$94.7 \pm 0.1 \text{ [dB]}$$

$$94.5$$

$$94.7$$

$$95.0$$

$$94.8$$

$$95.1$$

$$94.2$$

Table 12: One Way Propagation Path Data for 3.5 [V],
5000 [Hz] Continuous Wave Supply from the HP3314A
Function Generator; Collected 7 December 1987.

$$(V_{\text{rms}})_t = 0.523 \pm 0.001 \text{ [V]}$$

$$T_c \approx 21.0 \text{ [}^\circ\text{C]}$$

$$Rh \approx 50.0 \text{ [%]}$$

$$P = 1021.5 \pm 0.2 \text{ [mb]}$$

$$R = 5.30 \text{ [m]} \text{ (calculated from two way propagation path data for spheres two, three and four)}$$

$$I_r \text{ (referenced to } 10^{-12} \text{ [W/m}^2\text{])}$$

$$97.4 \pm 0.1 \text{ [dB]}$$

$$96.4$$

$$95.1$$

$$97.0$$

$$96.2$$

$$97.1$$

$$96.4$$

$$95.4$$

$$96.3$$

$$97.4$$

LIST OF REFERENCES

1. Little, C. Gordon, "Acoustic Methods for the Remote Probing of the Lower Atmosphere," Proceedings of the IEEE, v. 57, pp. 571-578, April 1969.
2. "Science and the Citizen," Scientific American, p. 54, February 1986.
3. Yariv, Amnon, Optical Electronics, 3d ed., pp. 499-523, Holt, Rinehart and Winston, 1985.
4. Pinson, Lewis J., Electro-optics, pp. 193-217, John Wiley & Sons, 1985.
5. Wroblewski, Michael Raymond, Development of a Data Analysis System for the Detection of Lower Level Atmospheric Turbulence with an Acoustic Sounder, Master's Thesis, Naval Postgraduate School, Monterey, California, June 1987.
6. Weingartner, Frank Joseph, Development of an Acoustic Echosounder for Detection of Lower Level Atmospheric Turbulence, Master's Thesis, Naval Postgraduate School, Monterey, California, June 1987.
7. U.S. Department of Commerce National Oceanic and Atmospheric Administration Environmental Research Laboratories, Technical Report ERL 322-WPL 38, Quantitative Evaluation of Acoustic Echoes from the Planetary Boundary Layer, by William D. Neff, June 1975.
8. Moxcey, Louis Robert, Utilization of Dense Packed Planar Acoustic Echosounders to Identify Turbulence Structure in the Lowest Levels of the Atmosphere, Master's Thesis, Naval Postgraduate School, Monterey, California, December 1987.

9. Tatarski, V. I., The Effects of the Turbulent Atmosphere on Wave Propagation, U.S. Department of Commerce, Washington, D.C., 1971; available from National Technical Information Service, Springfield, Virginia 22161.
10. Skolnik, Merrill I., Introduction to Radar Systems, 2d ed., pp.15-35, 54-62, 65, McGraw-Hill Book Company, 1980.
11. Probert-Jones, J. R., "The Radar Equation in Meteorology," Quarterly Journal of the Royal Meteorology Society, v. 88, pp. 485-495, 1962.
12. Smith, Ralph J., Circuits, Devices, and Systems, 4h ed., pp. 212-213, John Wiley & Sons, 1984.
13. Neiburger, Morris, Edinger, J. G., and Bonner, W. D., Understanding Our Atmospheric Environment, 2d ed., pp. 114-120, W. H. Freeman and Company, 1982.
14. Fuller, Robert J., Parametric Analysis of Echosounder Performance, Master's Thesis, Naval Postgraduate School, Monterey, California, September 1985.
15. Fleagle, Robert G. and Businger, J. A., An Introduction to Atmospheric Physics, 2d ed. (International Geophysics Series, Vol. 25), pp.71-72, 197-199, 324-325, Academic Press, 1980.
16. Bowman, J. J., and others, Electromagnetic and Acoustic Scattering by Simple Shapes, pp. vii, 1-8, 17-20, 349-354, 369-376, North-Holland Publishing Company, 1969.
17. Morse, Philip M., Vibration and Sound, pp. 311-321, 346-357, American Institute of Physics, 1976.
18. Elton, L. R. B., Introductory Nuclear Theory, 2d ed., pp. 56-61, Sir Isaac Pitman and Sons Ltd., 1966.

19. Cohen-Tannoudji, Claude, Diu, Bernard, and Laloë, Franck, Quantum Mechanics, v. 2, pp. 903-912, 913-915, 921-936, John Wiley & Sons, 1977.
20. Lax, M., and Feshbach, H., "Absorption and Scattering for Impedance Boundary Conditions on Spheres and Circular Cylinders," The Journal of the Acoustical Society of America, v. 20 no. 2, pp. 108-123, March 1948.
21. Boas, Mary L., Mathematical Methods in the Physical Sciences, 2d ed., pp. 483-492, 495, 499-502, 509-518, John Wiley & Sons, 1983.
22. Messiah, Albert, Quantum Mechanics, v. 1, pp. 369-387, North-Holland Publishing Company, 1961.
23. Abramowitz, Milton, and Stegun, Irene A., Handbook of Mathematical Functions with Formulas, Graphs, and Mathematical Tables, pp. 437-440, U.S. Government Printing Office, December 1972.
24. Lentz, William J., "Generating Bessel Functions in Mie Scattering Calculations Using Continued Fractions," Applied Optics, v. 15 no. 3, pp. 668-671, March 1976.
25. U.S. Army Atmospheric Sciences Laboratory Report ASL-TR-0152, Simplified Continued Fraction Calculation of Spherical Bessel Functions, by W. J. Lentz, pp. 5-11, September 1984.
26. Walters, D. L., Naval Postgraduate School, Monterey, California, Personal Communication, 19 September 1988.

INITIAL DISTRIBUTION LIST

	No. of Copies
1. Defense Technical Information Center Cameron Station Alexandria, VA 22304-6145	2
2. Library, Code 0142 Naval Postgraduate School Monterey, CA 93943-5002	2
3. Prof. Donald L. Walters Department of Physics (Code 61We) Naval Postgraduate School Monterey, CA 93943-5004	5
4. Prof. Anthony Atchley Department of Physics (Code 61Ay) Naval Postgraduate School Monterey, CA 93943-5004	1
5. Prof. Steven L. Garrett Department of Physics (Code 61Gt) Naval Postgraduate School Monterey, CA 93943-5004	1
6. Prof. Brian Wilson Department of Physics (Code 61W1) Naval Postgraduate School Monterey, CA 93943-5004	2

- | | | |
|----|---|---|
| 7. | Mr. William J. Lentz
Department of Physics (Code 61Cr)
Naval Postgraduate School
Monterey, CA 93943-5004 | 2 |
| 8. | Prof. Karlheinz E. Woehler
Chairman, Department of Physics (Code 61Wh)
Naval Postgraduate School
Monterey, CA 93943-5004 | 1 |
| 9. | Commanding Officer
HSL-36
Naval Air Facility
Mayport, FL 32228
ATTN: Lt. D. Paul Davison, Jr. | 2 |

Thesis

D17486 Davison

c.1 An investigation into
backscattered cross sec-
tion calibration of an
acoustic sounder used
for analysis of lower
atmospheric turbulence.

Thesis

D17486 Davison

c.1 An investigation into
backscattered cross sec-
tion calibration of an
acoustic sounder used
for analysis of lower
atmospheric turbulence.



thesD17486

An investigation into backscattered cros



3 2768 000 81205 1

DUDLEY KNOX LIBRARY